

Domain-Adjusted Regression or: ERM May Already Learn Features Sufficient for Out-of-Distribution Generalization

Elan Rosenfeld¹ Pradeep Ravikumar¹ Andrej Risteski¹

Abstract

A common explanation for the failure of deep networks to generalize out-of-distribution is that they fail to recover the “correct” features. Focusing on the domain generalization setting, we challenge this notion with a simple experiment which suggests that ERM already learns sufficient features and that the current bottleneck is not feature learning, but *robust regression*. We therefore argue that devising simpler methods for learning predictors on existing features is a promising direction for future research. Towards this end, we introduce *Domain-Adjusted Regression* (DARE), a convex objective for learning a linear predictor that is provably robust under a new model of distribution shift. Rather than learning one function, DARE performs a domain-specific adjustment to unify the domains in a canonical latent space and learns to predict in this space. Under a natural model, we prove that the DARE solution is the minimax-optimal predictor for a constrained set of test distributions. Further, we provide the first finite-environment convergence guarantee to the minimax risk, improving over existing results which show a “threshold effect”. Evaluated on finetuned features, we find that DARE compares favorably to prior methods, consistently achieving equal or better performance.

1. Introduction

The historical motivation for deep learning focuses on the ability of deep neural networks to automatically learn rich, hierarchical features of complex data (LeCun et al., 2015; Goodfellow et al., 2016). Simple Empirical Risk Minimization (ERM), with appropriate regularization, results in high-quality representations which surpass carefully hand-selected features on a wide variety of downstream tasks. Despite these successes, or perhaps because of them, the

¹Machine Learning Department, Carnegie Mellon University. Correspondence to: Elan Rosenfeld <elan@cmu.edu>.

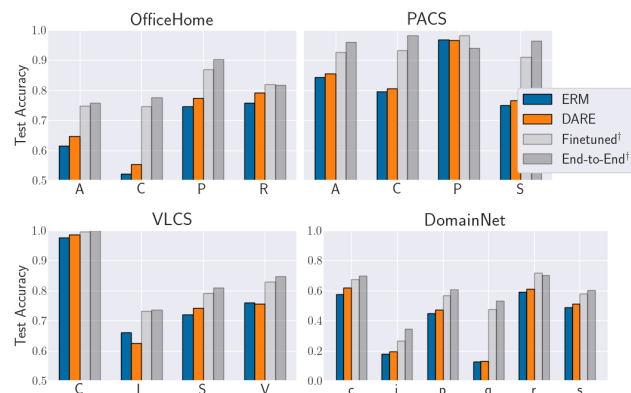


Figure 1. Accuracy via “cheating” (mean over 3 trials): dagger (†) denotes access to test domain at train-time. Each letter is a domain. Blue is approximate state of the art ERM, orange is our proposed DARE objective, light grey represents cheating while retraining the linear classifier only. All three methods use the *same features*, attained without cheating. Dark grey is “ideal” accuracy, cheating while training the entire deep network. Surprisingly, cheating only for the linear classifier rivals cheating for the whole network.

dominant focus of late is on the shortcomings of this approach: recent work points to the failure of networks trained with ERM to generalize under even moderate distribution shift (Recht et al., 2019; Miller et al., 2020). A common explanation for this phenomenon is reliance on “spurious correlations” or “shortcuts”, where a network makes predictions based on structure in the data which generalizes on average in the training set but may not persist in future test distributions (Poliak et al., 2018; Kaushik & Lipton, 2018; Geirhos et al., 2019; Xiao et al., 2021).

Many proposed solutions *implicitly assume* that this problem is due to the entire neural network: they suggest an alternate objective to be minimized over a deep network in an end-to-end fashion (Sun & Saenko, 2016; Ganin et al., 2016; Arjovsky et al., 2019). These objectives are complex, poorly understood, and difficult to optimize. Indeed, the efficacy of many such objectives was recently called into serious question (Zhao et al., 2019; Rosenfeld et al., 2021; Gulrajani & Lopez-Paz, 2021). Though a neural network is often viewed as a deep feature embedder with a final linear predictor applied to the features, it is still unclear—and to our knowledge *has not been directly asked or tested*—whether these issues are primarily because of (i) learning

the wrong features or (ii) learning good features but failing to find the best-generalizing linear predictor on top of them.

We begin with a simple experiment (Figure 1) to try to distinguish between these two possibilities: we train a deep network with ERM on several domain generalization benchmarks, where the task is to learn a predictor using a collection of distinct training domains and then perform well on a new, unseen domain. After training, we freeze the features and separately learn a linear classifier on top of them. Crucially, when training this classifier (i.e., retraining just the last linear layer), we give it an unreasonable advantage by optimizing on both the train and test domains—henceforth we refer to this as “cheating”. This process establishes a rough lower bound on what performance we could plausibly achieve using standard ERM features. We then separately cheat while training the full network end-to-end, simulating the idealized setting with no distribution shift. Note that in neither case do we train on the test *points*; our cheating entails training on (different) samples from the test *domain*, which are assumed unavailable in domain generalization.

Notably, we find that simple logistic regression on frozen deep features learned via ERM results in enormous improvements over current state of the art, on the order of 10-15%, and it usually performs comparably to the full cheating method—which learns both features and classifier end-to-end with test domain access—sometimes even outperforming it. Put another way, **cheating while training the entire network rarely does significantly better than cheating while training just the last linear layer**. This result suggests that the features learned by traditional ERM may be “good enough” and that the current bottleneck to out-of-distribution generalization lies primarily in the task of learning a simple, robust predictor.

Motivated by these findings, we propose a new invariance-based objective, which we call Domain-Adjusted Regression (DARE). The DARE objective is convex and it learns a linear predictor on frozen features. Unlike invariant prediction (Peters et al., 2016), which intentionally projects out variation in order to learn one predictor which performs acceptably on very different domains, DARE performs a domain-specific adjustment to unify the environments in a canonical latent space and learns to robustly predict in this space. Based on the presumption that standard ERM features are good enough (made formal in Section 4), DARE enjoys strong theoretical guarantees: under a new model of distribution shift which captures ideas from invariant/non-invariant latent variable models, we precisely characterize the adversarial risk of the DARE solution against a natural perturbation set, and we prove that this risk is *minimax*. The perturbation set consists of all test distributions where the adversary can introduce any change in directions in which the training domains already vary but is allowed only lim-

ited variation in new directions. We further provide the first finite-environment convergence guarantee to the minimax risk, improving over existing results which merely demonstrate a threshold at which the solution is discovered (Arjovsky et al., 2019; Rosenfeld et al., 2021; Chen et al., 2021). Finally, we show how our objective can be modified to leverage access to unlabeled samples at test-time; we use this to derive a provable method for “just-in-time” unsupervised domain adaptation for which we provide a finite-sample excess risk bound.

Evaluated on finetuned features, we find that DARE compares favorably to existing methods, consistently achieving equal or better performance. We also find that methods which previously underperformed on these benchmarks do much better in this setting, often besting ERM. This suggests that these approaches *are* beneficial for linear prediction (the setting in which they are understood and justified) but using them to train deep networks may result in worse features. We hope these results will encourage going “back to basics”, with future work focusing on simpler, easier to understand methods for robust prediction.

The concepts behind DARE have interesting connections to existing lines of work on robust regression under structural causal models (Rothenhäusler et al., 2021; Chen & Bühlmann, 2021), as well as “feature-matching” objectives (Ganin et al., 2016; Sun & Saenko, 2016) and those based on invariant prediction (Peters et al., 2016; Rojas-Carulla et al., 2018). We list related work in Section 7 and discuss some connections in greater detail in the Appendix.

2. ERM Learns Surprisingly Useful Features

Our experiments are motivated by a simple question: **is the observed failure of deep neural networks to generalize out-of-distribution more appropriately attributed to inadequate feature learning or inadequate robust prediction?** Both could undoubtedly be improved, but we are concerned with which currently serves as the primary bottleneck. It’s typical to train the entire network end-to-end and then evaluate on a test distribution; in reality, this measures the quality of the interaction of the features and the classifier, not of either one individually.

Using datasets and methodology from DOMAINBED (Gulrajani & Lopez-Paz, 2021), we finetune a ResNet-50 (He et al., 2016) with ERM on the training domains to extract features. Next, we cheat while learning a linear classifier on top of these frozen features by optimizing on both the train and test domains. We compare this classifier to a network which is trained on all domains end-to-end. If it is the case that ERM learns features which do not generalize,¹ we should expect

¹By this we mean that a linear predictor which approximately minimizes error on the train distribution will have large error on the test distribution.

that the linear classifier will not substantially improve over the current state of the art and will perform significantly worse than cheating end-to-end, since the latter method can adapt the features to better suit the test domain.

Instead, we find that simply giving the linear predictor access to all domains while training makes up the vast majority of the gap between current state of the art (ERM with heavy regularization) and the ideal setting. In other words, ERM produces features which are informative enough that a linear classifier on top of these frozen features is—in principle—capable of generalizing *almost as well as if we had access to the test domain when training the entire network*.² We observe a similar result using a pretrained network, though not for all domains and to a lesser degree. See Appendix E for additional experiments.

We conjecture that this phenomenon occurs more broadly: our findings suggest that for many applications, existing features learned via ERM may be “good enough” for out-of-distribution generalization in deep learning. That is, ERM may already “undo” a large component of the non-linearities we observe in complex data, even for unseen distributions. Two immediate questions are in which other settings this holds and if, instead of using more elaborate approaches such as complex regularization, the remaining gap could be closed using simpler, more robust classifiers. Based on this idea, we posit that future work would benefit from modularity, working to improve representation learning and robust classification/regression separately.³ There are several distinct advantages to this approach:

- **More robust comparisons and better reproducibility:** Current methods have myriad degrees of freedom which makes informative comparisons difficult; evaluating feature learning and robust regression separately eliminates many of these sources of experimental variation.
- **Less compute overhead:** Training large networks to learn both features and a classifier is expensive. Benchmarks could include files with the weights for ready-to-use deep feature embedders trained with various objectives—these models can be much larger and trained on much more data than would be feasible for many. Using these features, academic researchers could thus make faster progress on better classifiers with less compute.
- **Modular theoretical guarantees:** Conditioning on the frozen features, we can use more classical analyses to

²On a few domains the linear method sees a gap of $\sim 5\%$ accuracy from the idealized setting, and it may seem odd to refer to this as “comparable”. We emphasize that we use *attainable features*, learned with ERM on only the training domains, so this lower bounds the currently achievable error of a linear predictor: better performance is possible with a better classifier. The end-to-end result represents ideal performance that would a priori seem totally out of reach with current methods.

provide guarantees for the simpler parametric classifiers learned on top of these features. For example, Bansal et al. (2021) derive a generalization bound for simpler classifiers which is agnostic to the complexity of the frozen features on which they are trained.

We conclude by emphasizing that while the predictor in our experiments is linear, future methods need not be. Rather, we are highlighting that **there may be no need for complex, expensive, highly variable regularization of a deep network when much simpler approaches suffice**. We now describe one such approach.

3. The Domain-Adjusted Regression Objective

The goal of many prior methods in deep domain adaptation or generalization is to learn a single network which does well on all environments simultaneously, often by throwing away non-invariant components (Peng et al., 2019; Arjovsky et al., 2019). While invariance is a powerful framework, there are some clear drawbacks—in addition to explicitly ignoring possibly informative features, Zhao et al. (2019) show that marginal feature invariance cannot ensure generalization, and Stojanov et al. (2021) develop a toy setting where no single feature embedder can be sufficient.

Instead, we reframe the problem by thinking of each training domain as a distinct transformation from a shared canonical representation space. In this framing, we can “adjust” each domain in order to undo these transformations, aligning the representations to learn a single robust predictor in this unified space. Specifically, we propose to whiten each domain’s features to have zero mean and identity covariance, which can be thought of as a “domain-specific batchnorm” but using the full feature covariance. This idea is not totally new: some prior works align the moments between domains to improve generalization. The difference is that DARE does not learn a single featurizer which aligns the moments, but rather *aligns the moments of already learned features*; the latter approach maintains useful variation between domains which would be eliminated by the former.

DARE is closer to methods which learn separate batchnorm parameters per domain over a deep network, possibly adjusting at test-time (Seo et al., 2019; Chang et al., 2019; Segù et al., 2020)—these methods perform well, but they are entirely heuristic based, difficult to optimize, and come with no formal guarantees. Our theoretical analysis thus serves as preliminary justification for the observed benefits of such

³We are not suggesting an abandonment of the end-to-end framework; we believe both methods have merit. For example, the fact that the representation suffices does not imply that it corresponds to meaningful semantic features, and encouraging such a correspondence may depend on learning a system end-to-end.

methods, which have so far lacked serious grounding.

To begin, define \mathcal{E} as the set of observed training environments, each of which is defined by a distribution $p^e(x, y)$ over features $x \in \mathbb{R}^d$ and class labels $y \in [k]$. For each $e \in \mathcal{E}$, denote the mean and covariance of the features as μ_e, Σ_e . Our first step is to adjust the features via the whitening transformation $\Sigma_e^{-1/2}(x - \mu_e)$. If we believe that ERM is sufficient to recover a linear transformation of a ground-truth representation, whitening the data will then “undo” each domain’s unique transformation. Unfortunately, we cannot undo the test transformation because we have no way of knowing what the mean and covariance will be. Instead, we enforce that the mean of each training domain has *no effect* on our prediction, with the hope that this will result in the same invariance at test-time. Formally, the DARE objective finds a matrix $\beta \in \mathbb{R}^{d \times k}$ which solves

$$\begin{aligned} \min_{\beta} \quad & \sum_{e \in \mathcal{E}} \mathbb{E}_{p^e}[\ell(\beta^T \Sigma_e^{-1/2}(x - \mu_e), y)] \\ \text{s.t.} \quad & \text{softmax}(\beta^T \Sigma_e^{-1/2} \mu_e) = \frac{1}{k} \mathbf{1}. \quad \forall e \in \mathcal{E}, \end{aligned} \quad (1)$$

where ℓ is the multinomial logistic loss. For the special case of binary classification, β is a vector and the softmax is replaced with the logistic function $\sigma(x) = \frac{1}{1+e^{-x}}$.

Thus, the DARE objective explicitly regresses on the adjusted features, while the constraint enforces that in each environment the mean prediction contains no information about the class label (it must be uniform over the classes) to encourage our predictions to also be invariant to test-time transformations. The astute reader will point out that we also do not know the correct whitening matrix—instead, we adjust using our best guess for the test covariance: denoting this estimate as $\bar{\Sigma}$, our prediction on a new sample x at test-time is $f(x; \beta) = \text{softmax}(\beta^T \bar{\Sigma}^{-1/2} x)$. We prove that this prediction is minimax so long as our guess is “sufficiently close”, and in practice we find that simply averaging the training domain adjustments performs well. We expect future work could improve on this choice of $\bar{\Sigma}$.

Note that unlike many prior methods, DARE does *not* enforce invariance of the features themselves. In Section 5 we demonstrate that the DARE objective is in fact minimizing the worst-case risk under a constrained set of possible distribution shifts, and it is therefore less conservative than methods which require complete feature invariance.

Implementation in practice. Due to its convexity, the DARE objective is extremely simple to optimize. In practice, we finetune a deep network over the training data with ERM and then extract the features. Next, treating the frozen features of the training data as direct observations x , we

minimize the empirical Lagrangian form

$$\hat{\mathcal{L}}_{\text{cls}}^{\lambda}(\beta) := \frac{1}{|\mathcal{E}|} \sum_{e \in \mathcal{E}} \left[\frac{1}{n_e} \sum_{i=1}^{n_e} \ell(\beta^T \hat{\Sigma}_e^{-1/2}(x_i - \hat{\mu}_e), y_i) + \lambda \ell(\beta^T \hat{\Sigma}_e^{-1/2} \hat{\mu}_e, k^{-1} \mathbf{1}) \right],$$

where $\hat{\mu}_e, \hat{\Sigma}_e$ are the usual sample estimates and n_e is the number of samples in environment e . We define the “uncentered DARE objective” identically but without subtracting $\hat{\mu}_e$ in the first loss term. We found that the solution is incredibly robust to the choice of λ and that increasing λ beyond ~ 1 has practically no effect on loss or accuracy, though making it *much* larger (e.g. 10^5) can make optimization slower. Ablations can be found in Appendix E.

DARE for regression. For regression, we consider the same setup as (1) but with targets $y \in \mathbb{R}$. By the same reasoning, DARE minimizes error on the adjusted domains subject to the mean output having no effect on the prediction:

$$\begin{aligned} \min_{\beta} \quad & \sum_{e \in \mathcal{E}} \mathbb{E}_{p^e}[(\beta^T \Sigma_e^{-1/2}(x - \mu_e) - y)^2] \\ \text{s.t.} \quad & \beta^T \Sigma_e^{-1/2} \mu_e = 0. \quad \forall e \in \mathcal{E}. \end{aligned} \quad (2)$$

We define the empirical Lagrangian $\hat{\mathcal{L}}_{\text{reg}}^{\lambda}$ analogously to its classification counterpart. There is an interesting connection here to anchor regression (Rothenhäusler et al., 2021), which we expand on in Appendix A.1. We remark that if $|\mathcal{E}| \geq d$ and the means are in general position then the only solution is $\beta = 0$; but observing so many distinct environments is unrealistic, and furthermore if this does hold it is exactly the setting when ERM could be expected to succeed. We are therefore more concerned with the setting $|\mathcal{E}| \ll d$.

Leveraging unlabeled test samples. Another benefit to our approach is that the adjustments for each domain do not depend on labels, so given access to unlabeled samples from the test domain we can make a more informed estimate. In this case, it is preferable to solve (1) without the constraint and use the empirical test covariance for $\bar{\Sigma}$. Such access occurs in the setting of unsupervised domain adaptation, but unlike methods which use those samples while training, this adjustment can be done *even if the samples are only available test-time*. We name this task *Just-in-Time Unsupervised Domain Adaptation* (JIT-UDA), and we provide finite-sample risk bounds for the DARE objective in this setting. We believe JIT-UDA presents a promising direction for future theoretical research: it is much weaker—and arguably more realistic—to assume access to unlabeled samples only at test-time. JIT-UDA is also amenable to analyses beyond worst-case, such as minimizing regret when observing test data sequentially (Rosenfeld et al., 2022). There exist works

which use unlabeled samples at test-time to improve performance (see Sun et al. (2020) and references therein), but to our knowledge this is the first work to formally establish and analyze this setting. A few prior works solve the task implicitly via a kernel on the test data (Blanchard et al., 2011; Muandet et al., 2013; Deshmukh et al., 2019), but this computation scales with both the train and test datasets and it must be repeated whenever new data is obtained. Their bounds also assume a prior over domains and so they do not allow for a minimax analysis.

4. A New Model of Distribution Shift

The DARE objective is based on the intuition that all domains jointly share a representation space and that they arise as unique transformations from this space. To capture this notion mathematically, we model the joint distribution $p^e(\epsilon, y)$ over latents $\epsilon \in \mathbb{R}^d$ and label $y \in \{0, 1\}$, along with an environment-specific transformation to observations $x \in \mathbb{R}^d$ for each domain. In the fully general case, this transformation can take an arbitrary form and can be written as $x = T_e(\epsilon, y)$.

Our primary assumption is that $p^e(y \mid \epsilon)$ is constant for all domains—our goal is thus to invert each transformation T_e such that for all domains we are learning the same conditional $p(y \mid T_e^{-1}(x))$ (throughout we assume T_e is invertible). One can also view this model as a generalization of covariate shift: where the usual assumption is constancy of $p(y \mid x)$, our inclusion of the inverse transformation gives a richer model which can more realistically capture real-world variation across domains. For example, the T_e could correspond to different image “styles”; we then would hope to learn to eliminate individual style variations.

For a typical deep learning analysis we would model T_e as a complex non-linear generative map from latents to high-dimensional observations. However, our finding that ERM features are good enough suggests that modeling T_e as a simple function is not unreasonable. We therefore restrict our analysis to the setting where x is a linear function of ϵ . For classification, we consider the following model:

$$\epsilon = \epsilon_0 + b_e, y = \mathbf{1}\{\beta^{*T}\epsilon + \eta \geq 0\}, x = A_e\epsilon. \quad (3)$$

Here, $\epsilon_0 \in \mathbb{R}^d \sim p^e(\epsilon_0)$, which we allow to be *any domain-specific distribution*; we assume only that its mean is zero (such that $\mathbb{E}[\epsilon] = b_e$) and that its covariance exists. We fix $\beta^* \in \mathbb{R}^d$ for all domains and model η as logistic noise. Finally, $A_e \in \mathbb{R}^{d \times d}$, $b_e \in \mathbb{R}^d$ are domain-specific constants. For regression, we model the same generative process except we let $y \in \mathbb{R}$ and η is arbitrary zero-mean independent noise, i.e. $y = \beta^{*T}\epsilon + \eta$. We remark that the reason for separate definitions of $p^e(\epsilon_0)$ and b_e is that our robustness guarantees are agnostic to the distribution of latent residuals $p^e(\epsilon_0)$ —the *only* aspect of the latent distribution $p(\epsilon)$ which affects our bounds is the environment mean b_e .

Connection to Invariant Prediction. Statistical models of varying and invariant latent features have recently become a popular tool for analyzing the behavior of deep representation learning algorithms (Rosenfeld et al., 2021; Chen et al., 2021; Wald et al., 2021). We see that (3) can model such a setting by assuming, e.g., that a subspace of the columnspan of A_e is constant for all e , while the remaining subspace can vary arbitrarily. This would imply that the minimax-optimal prediction must throw away the varying subspace. Instead, DARE *realigns* the subspaces so that we can use them at test-time. We illustrate this with the following running example:

Example 1 (Invariant Prediction vs. Domain-Adjusted Regression). Consider the model (3) with $\epsilon \sim \mathcal{N}(0, I_{d_1+d_2})$.

Define $\Pi := \begin{bmatrix} I_{d_1} & \mathbf{0} \\ \mathbf{0} & \mathbf{0}_{d_2} \end{bmatrix}$ and assume $A_e = \begin{bmatrix} \Sigma^{1/2} & \mathbf{0} \\ \mathbf{0} & \Sigma_e^{1/2} \end{bmatrix}$ for all e , where $\Sigma \in \mathbb{R}^{d_1 \times d_1}$ is constant for all domains but $\Sigma_e \in \mathbb{R}^{d_2 \times d_2}$ varies.

Here we have a simple latent variable model which captures the same intuition as that of Rosenfeld et al. (2021): a subspace of the observations (i.e., $\text{span}(\Pi)$) has an invariant relationship with the target. The goal of an invariant prediction algorithm such as IRM (Arjovsky et al., 2019) would be to learn the featurizer Φ which is minimax-optimal; in this case, the solution is $\Phi(x) = \begin{bmatrix} \Sigma^{-1/2} & \mathbf{0} \\ \mathbf{0} & \mathbf{0} \end{bmatrix} x$. This Φ retains only the component lying in $\text{span}(\Pi)$, because our ability to predict y with this subspace is invariant. Such a predictor is often unnecessarily conservative, as we may expect that for a future distribution $\Sigma_{e'} = (I - \Pi)A_{e'}(I - \Pi)$ will not be *too* different from what we have seen before. DARE takes advantage of this possibility, and we will shortly see the resulting benefits.

5. Theoretical Analysis

Before we can analyze the DARE objective, we observe that there is a fundamental unidentifiability in (3), since two identical observational distributions $p(x, y)$ can have different regression vectors β^* . This would prevent all domains from sharing an optimal predictor, which is precisely what our model assumes. We therefore begin with a simple assumption which ensures identifiability:

Assumption 5.1. Write the SVD of A_e as $U_e S_e V_e^T$. We assume $V_e = V \forall e$.

One special case where this holds is when A_e is constant for all domains; this is very similar to the “additive intervention” setting of Rothenhäusler et al. (2021), since only p^e, b_e can vary. We assume WLOG that $V = I$, as any other value can be subsumed by the other parameters. We further let $\mathbb{E}[\epsilon_0 \epsilon_0^T] = I$ WLOG by the same reasoning. With Assumption 5.1, we can uniquely recover $A_e = U_e S_e$ via the eigen-

decomposition of the covariance $\Sigma_e = A_e A_e^T = U_e S_e^2 U_e^T$. We therefore use the notation $\Sigma_e^{1/2}$ to refer to A_e recovered in this way. We allow covariances to have zero eigenvalues, in which case we write the matrix inverse to implicitly refer to the pseudoinverse. As is standard in domain generalization analysis, unless stated otherwise we assume full distribution access to the training domains, though standard concentration inequalities could easily be applied.

We begin by deriving the solution to Equations (1) and (2) for any set of training domains we might optimize over. Recall that the DARE constraint requires that the mean representation of each domain has no effect on our prediction. To enforce this, the DARE solution must project out the subspace in which the means vary. Given a set of E training environments, define \mathbb{B} as the $d \times E$ matrix whose columns are the environmental mean parameters b_e . Throughout this section, we make use of the matrix $\hat{\Pi}$, which is defined as the orthogonal projection onto the nullspace of \mathbb{B}^T : $\hat{\Pi} := I - \mathbb{B}\mathbb{B}^\dagger = U_{\hat{\Pi}} S_{\hat{\Pi}} U_{\hat{\Pi}}^T \in \mathbb{R}^{d \times d}$. This matrix projects onto the DARE constraint set, and it turns out to be all that is necessary to state the solution:

Theorem 5.2. (Closed-form solution to the DARE population objective). *Under model (3), the solution to the DARE population objective (2) for linear regression is $\hat{\Pi}\beta^*$. If ϵ is Gaussian, then the solution for logistic regression (1) is $\alpha\hat{\Pi}\beta^*$ for some $\alpha \in (0, 1]$.*

The intuition behind the proof is as follows: due to the constraint, the centered DARE objective is equivalent to the uncentered objective—for the latter, the excess risk of a vector $\hat{\beta}$ is $\mathbb{E}[(\hat{\beta}^T \epsilon - \beta^{*T} \epsilon)^2] = \|\hat{\beta} - \beta^*\|^2$. Therefore, the solution is the ℓ_2 -projection of β^* onto the constraint set, which is precisely $\hat{\Pi}\beta^*$.

Remark 5.3. In Example 1, we saw how invariant prediction will often discard a large subspace of the representation and why this is undesirable. Instead, DARE undoes the environment transformation and regresses directly on $\epsilon = T_e^{-1}(x)$. Because we are performing a separate transformation for each environment, we are *aligning* the varying subspaces rather than throwing them away, allowing us to make use of additional information. Though the DARE solution also recovers β^* up to a projection, it is using the adjusted features; DARE therefore only removes what cannot be aligned. In particular, whereas Π has rank d_1 in Example 1, $\hat{\Pi} = I$ would have full rank. This retains strictly more information: if we expect worst-case distribution shift we can still project to the invariant subspace, but if not then we can often perform much better. Indeed, in the ideal setting where we have a good estimate of $\Sigma_{e'}$ (e.g., under mild distribution shift or when solving JIT-UDA), we can make the Bayes-optimal prediction as $\mathbb{E}[y | x] = \beta^{*T} A_{e'}^{-1} x$. Thus we see a clear advantage that DARE enjoys over invariant prediction.

The second result of Theorem 5.2 depends on a key lemma about the closed-form solution to a projection-constrained logistic regression problem, which we state and prove as Lemma B.1 in the Appendix. The result is somewhat general and we expect it could be of independent interest, yet we found surprisingly few related results in the literature. Though we prove this lemma only for Gaussian z , we found empirically that the result approximately holds whenever z is dimension-wise independent and symmetric about the origin, likely as a consequence of the Central Limit Theorem (see discussion in the Appendix).

5.1. The Adversarial Risk of DARE

Moving forward, we denote the DARE solution $\beta_{\hat{\Pi}}^* := \hat{\Pi}\beta^*$, with $\beta_{I-\hat{\Pi}}^*$ defined analogously. We next study the behavior of the DARE solution under worst-case distribution shift. We consider the setting where an adversary directly observes our choices of $\bar{\Sigma}$, $\hat{\beta}$ and chooses new environmental parameters $A_{e'}$, $b_{e'}$ so as to cause the greatest possible loss. Specifically, we study the square loss, defining the *excess* test risk of a predictor as $\mathcal{R}_{e'}(\hat{\beta}) := \mathbb{E}_{p_{e'}}[(\hat{\beta}^T \bar{\Sigma}^{-1/2} x - \beta^{*T} \epsilon)^2]$ (we leave the dependence on $\bar{\Sigma}$ implicit). For logistic regression we therefore analyze the squared error with respect to the log-odds. With some abuse of notation, we also reference excess risk when only using a particular subspace, i.e. $\mathcal{R}_{e'}^{\Pi}(\hat{\beta}) := \mathbb{E}_{p_{e'}}[(\hat{\beta}^T \bar{\Sigma}^{-1/2} x - \beta_{\Pi}^{*T} \epsilon)^2]$.

Because we guess $\bar{\Sigma}$ before observing any data from this new distribution, ensuring success is impossible in the general case. Instead, we consider a set of restrictions on the adversary which will make the problem tractable. Define the error in our test domain adjustment as $\Delta := \Sigma_{e'}^{1/2} \bar{\Sigma}^{-1/2} - I$; observe that if $\bar{\Sigma} = \Sigma_{e'}$, then $\Delta = 0$. Our first assumption³ says that the effect of our adjustment error with respect to the *interaction between subspaces* $\hat{\Pi}$ and $(I - \hat{\Pi})$ is bounded:

Assumption 5.4 (Approximate recovery of subspaces). For a fixed constant $B \geq 0$, $\|(I - \hat{\Pi})\Delta\hat{\Pi}\hat{\beta}\| \leq B\|\hat{\Pi}\beta^*\|$.

Remark 5.5. To see specific cases when this would hold, consider the decomposition of Δ according to its components in the subspaces $\hat{\Pi}$ and $I - \hat{\Pi}$:

$$U_{\hat{\Pi}}^T \Delta U_{\hat{\Pi}} = \begin{bmatrix} \Delta_1 & \Delta_{12} \\ \Delta_{21} & \Delta_2 \end{bmatrix},$$

where $\Delta_1 \in \mathbb{R}^{\text{rank}(\hat{\Pi}) \times \text{rank}(\hat{\Pi})}$. A few settings automatically satisfy Assumption 5.4 with $B = 0$, due to the fact that $U_{\hat{\Pi}}^T \Delta U_{\hat{\Pi}}$ will be block-diagonal. In particular, this will be the case if all domains share an invariant subspace—e.g., if $\Pi A_e \Pi$ is constant as in Example 1. Below, we show that in this setting, exact recovery of this subspace occurs once we observe $\text{rank}(I - \Pi)$ environments—this matches

³Though we label these as assumptions, they are properly interpreted as *restrictions* on an adversary—we consider an “uncertainty set” comprising all possible domains subject to these requirements.

(actually, it is one less than) the linear environment complexity of most invariant predictors (Rosenfeld et al., 2021), and therefore Assumption 5.4 with $B = 0$ is no stronger than assuming a linear number of environments. This will similarly occur if U_e is shared across all environments (e.g., under fixed A_e as described above) and we use any sort of “averaging” guess of $\bar{\Sigma}$.

Our second assumption concerns the magnitude of our error in the non-varying subspace:

Assumption 5.6 (Bound on adjustment error in non-varying subspace). Using only covariates in the non-varying subspace, the risk of the ground truth regressor β^* is less than that of the trivial zero predictor: $\mathcal{R}_{p_{e'}}^{\hat{\Pi}}(\beta^*) < \mathcal{R}_{p_{e'}}^{\hat{\Pi}}(\mathbf{0})$.

The need for this restriction should be immediate—if our adjustment error were so large that this did not hold, even the oracle regression vector would do worse than simply always predicting $\hat{y} = 0$. Assumption 5.6 is satisfied for example if $\|\Delta\hat{\Pi}\| < 1$, which again is guaranteed if there is an invariant subspace. Note that we make *no restriction* on the risk in the subspace $I - \hat{\Pi}$ —the adversary is allowed any amount of variation in directions where we have *already seen* variation in the mean terms b_e , but introduction of *new* variation is assumed bounded. This is a no-free-lunch necessity: if we have never seen a particular type of variation, we cannot possibly know how to use it at test-time.

With these restrictions on the adversary, our main result derives the supremum of the excess test risk of the DARE solution under adversarial distribution shift. Furthermore, we prove that this risk is *minimax*: making no more restrictions on the adversary other than a global bound on the mean, the DARE solution achieves the best performance we could possibly hope for at test-time:

Theorem 5.7 (DARE risk and minimaxity). *For any $\rho \geq 0$, denote the set of possible test environments \mathcal{A}_ρ which contains all parameters $(A_{e'}, b_{e'})$ subject to Assumptions 5.4 and 5.6 and a bound on the mean: $\|b_{e'}\| \leq \rho$. For logistic or linear regression, let $\hat{\beta}$ be the minimizer of the corresponding DARE objective as in Theorem 5.2. Then,*

$$\sup_{(A_{e'}, b_{e'}) \in \mathcal{A}_\rho} \mathcal{R}_{e'}(\hat{\beta}) = (1 + \rho^2)(\|\beta^*\|^2 + 2B\|\beta_{\hat{\Pi}}^*\|\|\beta_{I-\hat{\Pi}}^*\|).$$

Furthermore, the DARE solution is minimax:

$$\hat{\beta} \in \arg \min_{\beta \in \mathbb{R}^d} \sup_{(A_{e'}, b_{e'}) \in \mathcal{A}_\rho} \mathcal{R}_{e'}(\beta).$$

Proof sketch. We decompose the excess risk into error on the target mean $\beta^{*T}b_{e'}$ and error on the residuals $\beta^{*T}\epsilon_0$, bounding the two separately. To show $\hat{\beta}$ is minimax, we construct a series of adversarial choices of $A_{e'}, b_{e'}$ which force larger risk for any predictor which does not satisfy certain properties. These properties progressively eliminate

possible predictors until all those which remain have the same adversarial risk as $\hat{\beta}$. \square

A special case when our assumptions hold is when all domains share an invariant subspace and we only predict using that subspace, but this is often too conservative. There are settings where allowing for (limited) new variation can improve our predictions, and Theorem 5.7 shows that DARE should outperform invariant prediction in such settings.

5.2. The Environment Complexity of DARE

An important new measure of domain generalization algorithms is their *environment complexity*, which describes how the test risk behaves as a function of the number of (possibly random) domains we observe. In contrast to Example 1, for this analysis we assume an invariant subspace Π outside of which *both* A_e and b_e can vary arbitrarily—we formalize this as a prior over the b_e whose covariance has the same span as $I - \Pi$. Thus the minimax vector is $\Pi\beta^*$ even after adjustment, so we can directly compare DARE to existing invariant prediction methods. Our next result demonstrates that DARE achieves the same threshold as prior methods, but we also prove the first *finite-environment convergence guarantee*, quantifying how quickly the risk of the DARE predictor approaches that of the minimax-optimal predictor. We define two quantities which appear in our bound, followed by the statement itself:

Definition 5.8. The *effective rank* of a matrix Σ is defined as $r(\Sigma) := \frac{\text{Tr}(\Sigma)}{\|\Sigma\|}$ and satisfies $1 \leq r(\Sigma) \leq \text{rank}(\Sigma)$.

Definition 5.9. Denote the eigenvalues in descending order as $\lambda_1 \geq \dots \geq \lambda_d$. We define the smallest gap between consecutive eigenvalues: $\xi(\Sigma) := \min_{i \in [d-1]} \lambda_i - \lambda_{i+1}$.

Theorem 5.10 (Environment complexity of DARE). *Fix test environment parameters $A_{e'}, b_{e'}$ and our guess $\bar{\Sigma}$. Suppose we minimize the DARE regression objective (2) on environments whose means b_e are Gaussian vectors with covariance Σ_b , with $\text{span}(\Sigma_b) = \text{span}(I - \Pi)$. After seeing E training domains:*

1. *If $E \geq \text{rank}(\Sigma_b)$ then DARE recovers the minimax-optimal predictor almost surely: $\hat{\beta} = \beta_{\Pi}^*$.*

2. *Otherwise, if $E \geq r(\Sigma_b)$ then with probability $\geq 1 - \delta$,*

$$\mathcal{R}_{e'}(\hat{\beta}) \leq \mathcal{R}_{e'}(\beta_{\Pi}^*) + \mathcal{O}\left(\frac{\|\Sigma_b\|}{\xi(\Sigma_b)} \left(\sqrt{\frac{r(\Sigma_b)}{E}} + \max\left\{ \sqrt{\frac{\log 1/\delta}{E}}, \frac{\log 1/\delta}{E} \right\} \right) \right),$$

where $\mathcal{O}(\cdot)$ hides dependence on $\|\Delta\|$.

For coherence we present the first item as a probabilistic statement, but it holds deterministically so long as there are $\text{rank}(\Sigma_b)$ linearly independent observations of b_e .

Proof sketch. The proof analyzes the error in our recovery of the correct subspace $\|\Pi - \hat{\Pi}\|$. Item 1 is immediate, as

Domain-Adjusted Regression

Dataset / Algorithm	Mean Accuracy by Domain ($\pm 90\%$ CI)				Dataset / Algorithm	Mean Accuracy by Domain ($\pm 90\%$ CI)					
Office-Home (Venkateswara et al., 2017)	A	C	P	R	VLC5 (Fang et al., 2013)	C	L	S	V		
ERM	61.4 \pm 1.9	52.1 \pm 1.6	74.6 \pm 0.7	75.8 \pm 1.9	ERM	97.6 \pm 0.7	66.1 \pm 0.6	71.9 \pm 1.9	76.1 \pm 2.3		
IRM	62.1 \pm 1.5	53.2 \pm 1.7	75.2 \pm 0.9	77.3 \pm 0.8	IRM	<u>98.6 \pm 0.6</u>	64.9 \pm 0.9	72.9 \pm 0.7	74.1 \pm 2.1		
GroupDRO	62.5 \pm 0.5	53.1 \pm 1.7	<u>75.7 \pm 0.5</u>	<u>77.7 \pm 1.1</u>	GroupDRO	<u>98.5 \pm 0.7</u>	65.0 \pm 0.5	73.9 \pm 1.0	75.1 \pm 1.8		
GroupERM	62.5 \pm 0.8	52.5 \pm 2.3	<u>75.7 \pm 0.5</u>	<u>77.4 \pm 0.8</u>	GroupERM	<u>98.6 \pm 0.7</u>	65.5 \pm 0.5	73.4 \pm 0.3	74.9 \pm 1.7		
DARE	64.7 \pm 0.8	55.4 \pm 1.1	77.5 \pm 0.3	79.2 \pm 0.5	DARE	<u>98.5 \pm 0.2</u>	62.5 \pm 1.6	74.3 \pm 1.4	75.5 \pm 1.4		
PACS (Li et al., 2017)	A	C	P	S	DomainNet (Peng et al., 2019)	c	i	p	q	r	s
ERM	84.3 \pm 1.5	79.5 \pm 1.9	96.7 \pm 0.5	74.9 \pm 3.7	ERM	57.6 \pm 0.6	17.9 \pm 0.6	44.7 \pm 0.7	12.6 \pm 0.9	59.0 \pm 0.7	48.6 \pm 0.3
IRM	83.6 \pm 0.4	79.2 \pm 0.5	97.1 \pm 0.2	76.4 \pm 2.3	IRM	<u>60.9 \pm 0.4</u>	<u>19.3 \pm 0.2</u>	<u>47.6 \pm 0.4</u>	12.4 \pm 0.4	<u>61.9 \pm 1.0</u>	<u>49.8 \pm 0.6</u>
GroupDRO	83.6 \pm 1.0	79.1 \pm 0.2	96.9 \pm 0.3	<u>76.8 \pm 2.8</u>	GroupDRO	57.8 \pm 0.7	<u>18.8 \pm 0.4</u>	<u>45.3 \pm 0.4</u>	11.9 \pm 0.8	59.5 \pm 1.0	47.9 \pm 0.9
GroupERM	83.6 \pm 1.0	78.8 \pm 0.2	97.1 \pm 0.3	76.5 \pm 2.3	GroupERM	<u>61.0 \pm 0.4</u>	19.1 \pm 0.4	<u>47.4 \pm 0.4</u>	12.3 \pm 0.6	<u>61.8 \pm 1.1</u>	<u>49.9 \pm 0.5</u>
DARE	85.6 \pm 0.6	80.5 \pm 1.0	96.6 \pm 0.4	76.7 \pm 2.0	DARE	61.7 \pm 0.2	<u>19.3 \pm 0.1</u>	<u>47.4 \pm 0.5</u>	13.1 \pm 0.7	<u>61.2 \pm 1.3</u>	51.4 \pm 0.3

Table 1. Performance of linear predictors on top of fixed features learned via ERM. Because all algorithms use the same set of features for each trial, results are not independent. Therefore, **bold** indicates highest mean according to one-sided paired t-tests at $p = 0.1$ significance. If not the overall highest, underline indicates higher mean than ERM under the same test.

under this condition we have $\|\Pi - \hat{\Pi}\| = 0$. For item 2, we show how to bound $\mathcal{R}_{e'}(\hat{\beta}) - \mathcal{R}_{e'}(\beta_{\Pi}^*)$ as $\mathcal{O}(\|\Pi - \hat{\Pi}\|)$. We then invoke a variant of the Davis-Kahan theorem plus a spectral concentration inequality to derive the result. \square

Remark 5.11. Prior analyses of invariant prediction methods only show a discontinuous threshold where the minmax predictor is discovered after seeing a fixed number of environments—usually linear in the non-invariant latent dimension—and DARE achieves a slightly better threshold. But one might expect that if the variation of environmental parameters is not *too* large then we can do better, and indeed Theorem 5.10 shows that if the *effective rank* of Σ_b is sufficiently small, the risk of the DARE predictor will approach that of the minimax predictor at a rate of $\mathcal{O}(E^{-1/2})$.

5.3. Applying DARE to JIT-UDA

So far, we have only considered a setting with no knowledge of the test domain. As discussed in Section 3, we’d expect that estimating the adjustment via unlabeled samples will improve performance. Prior works have extensively explored how to leverage access to unlabeled test samples for improved generalization—but while some suggest ways of using unlabeled samples “just-in time” (i.e., only at test-time), the advantages have not been formally quantified.

Our final theorem investigates the provable benefits of using the empirical moments instead of enforcing invariance, giving a finite-sample convergence guarantee for the unconstrained DARE objective in the JIT-UDA setting:

Theorem 5.12 (JIT-UDA, shortened). *Define $m(\Sigma) := \frac{\lambda_{\max}(\Sigma)}{\lambda_{\min}^3(\Sigma)}$. Assume the data follows the model (3) and that we observe $n_s = \Omega(m(\Sigma_S)d^2)$ samples from source distribution $\mathcal{N}(\mu_S, \Sigma_S)$ and $n_T = \Omega(m(\Sigma_T)d^2)$ samples from target distribution $\mathcal{N}(\mu_T, \Sigma_T)$. Suppose we solve for $\hat{\beta}$ which minimizes the unconstrained, uncentered objective $\hat{\mathcal{L}}_{\text{reg}}^0$ over the source data and predict $\hat{\beta}^T \hat{\Sigma}_T^{-1/2} x$ on the target data. Then with probability at least $1 - 3d^{-1}$, the excess squared risk of our predictor on the new environment is bounded as $\mathcal{R}_T(\hat{\beta}) = \mathcal{O}\left(d^2 \|\mu_T\|^2 \left(\frac{m(\Sigma_S)}{n_s} + \frac{m(\Sigma_T)}{n_T}\right)\right)$.*

Our proof readily applies to general sub-Gaussian distributions (the full theorem statement can be found in the Appendix). Experimentally, we found that DARE does not outperform methods specifically intended for UDA, possibly due to the fact that $n \ll d^2$ —but we believe this is a promising direction for future theoretical research, since it doesn’t require unlabeled samples at train-time and it can incorporate new data in a streaming fashion.

6. Experiments

Most algorithms implemented in the DOMAINBED benchmark are only applicable to deep networks; many apply complex regularization to either the learned features or the network itself. We instead compare to three popular algorithms which work for linear classifiers: ERM (Vapnik, 1999), IRM (Arjovsky et al., 2019), and GroupDRO (Sagawa et al., 2020). We also discovered that **simply rescaling ERM by downweighting each domain proportionally to its size serves as a strong additional baseline**. Concurrent work makes a similar observation, exploring this baseline when training the whole network rather than just the last layer (Idrissi et al., 2021). We denote this method “GroupERM” and we include it in our reported results in Table 1. We observe that GroupERM is equivalent to IRM with $\lambda = 0$, yet it almost always matches or outperforms IRM with $\lambda \neq 0$, implying that the observed benefit from IRM may be due mostly to the rescaling.

We evaluate all approaches on four datasets and we see that DARE consistently matches or surpasses prior methods. The features for each trial are the result of the default hyperparameter sweep of DOMAINBED; for computational reasons, we used fewer random hyperparameter choices per trial, meaning the reported accuracies are not directly comparable. Nevertheless, our results are significant because they are consistently evaluated according to the same methodology. Further implementation details can be found in Appendix D, along with ablations in Appendix E.

All algorithms use the same set of features for each trial, so their performances are highly dependent. To account

for this, we perform a one-sided paired t-test between algorithms to determine the best performers. The fact that DARE consistently bests ERM is somewhat surprising: it is intended to guard against a worst-case distribution shift and depends on the quality of our guess $\bar{\Sigma}$, so we would in general expect worse performance on some datasets. In future work we hope to further investigate in which settings DARE can be expected to over- or underperform.

Prior methods now consistently outperform ERM. It is interesting that the previously observed gap between ERM and alternatives disappears in this experimental setting. For example, [Gulrajani & Lopez-Paz \(2021\)](#) report IRM and GroupDRO performing much worse on DomainNet—5-10% lower accuracy on some domains—but they surpass ERM when using finetuned features. This could be because they learn worse features, or perhaps they are just more difficult to optimize over a deep network. This further motivates work on methods for learning simpler robust predictors.

7. Related Work

A popular approach to domain generalization matches the domains in feature space, either by aligning moments ([Sun & Saenko, 2016](#)) or with an adversarial loss ([Ganin et al., 2016](#)). DARE differs from these approaches in that the constraint requires only that the *feature mean projection onto the vector β* be invariant. The idea of a domain-invariant projection ([Baktashmotlagh et al., 2013](#)) was recently analyzed by [Chen & Bühlmann \(2021\)](#), though notably under fully observed features and only for domain adaptation. They analyze other invariances as well, and we expect combining these methods with domain adjustment can serve as an interesting direction for future study.

There has been intense recent focus on invariant prediction, based on ideas from causality ([Peters et al., 2016](#)) and catalyzed by IRM ([Arjovsky et al., 2019](#)). Though the goal of such methods is minimax-optimality under major distribution shift, later work identifies critical failure modes of this approach ([Rosenfeld et al., 2021](#); [Kamath et al., 2021](#)). As discussed in [Example 1](#), these methods eliminate features whose information is not invariant, which is often overly conservative. DARE instead allows for *limited* new variation by aligning the non-invariant subspaces, enabling stronger theoretical guarantees.

Some prior works “normalize” each domain by learning separate batchnorm parameters but sharing the rest of the network. Initially suggested for UDA ([Li et al., 2016](#); [Bousmalis et al., 2016](#); [Chang et al., 2019](#)), this idea has also been applied to domain generalization ([Seo et al., 2019](#); [Segù et al., 2020](#)) but in a somewhat ad-hoc manner—this is problematic because deep domain generalization methods were recently called into question when [Gulrajani & Lopez-](#)

[Paz \(2021\)](#) gave convincing evidence that no method beats ERM when evaluated fairly. Nevertheless, our analysis provides an initial justification for these methods, suggesting that this idea is worth exploring further.

Acknowledgements

We thank Arun Kumar Kuchibhotla for identifying an error in an earlier version of [Lemma B.1](#), as well as pointing us to the work of [Li & Duan \(1989\)](#). We are grateful to Saurabh Garg, Jeremy Cohen, Zack Lipton, and Siva Balakrishnan for helpful comments.

References

- Arjovsky, M., Bottou, L., Gulrajani, I., and Lopez-Paz, D. Invariant risk minimization. *arXiv preprint arXiv:1907.02893*, 2019.
- Baktashmotlagh, M., Harandi, M. T., Lovell, B. C., and Salzmann, M. Unsupervised domain adaptation by domain invariant projection. In *2013 IEEE International Conference on Computer Vision*, pp. 769–776, 2013. doi: 10.1109/ICCV.2013.100.
- Bansal, Y., Kaplun, G., and Barak, B. For self-supervised learning, rationality implies generalization, provably. In *International Conference on Learning Representations*, 2021.
- Blanchard, G., Lee, G., and Scott, C. Generalizing from several related classification tasks to a new unlabeled sample. In *Advances in Neural Information Processing Systems*, volume 24. Curran Associates, Inc., 2011.
- Bousmalis, K., Trigeorgis, G., Silberman, N., Krishnan, D., and Erhan, D. Domain separation networks. In *Proceedings of the 30th International Conference on Neural Information Processing Systems, NIPS’16*, pp. 343–351, Red Hook, NY, USA, 2016. Curran Associates Inc. ISBN 9781510838819.
- Carlsson, M. Perturbation theory for the matrix square root and matrix modulus. 10 2018.
- Chang, W.-G., You, T., Seo, S., Kwak, S., and Han, B. Domain-specific batch normalization for unsupervised domain adaptation. *arXiv preprint arXiv:1906.03950*, 2019.
- Chen, Y. and Bühlmann, P. Domain adaptation under structural causal models. *Journal of Machine Learning Research*, 22(261):1–80, 2021.
- Chen, Y., Rosenfeld, E., Sellke, M., Ma, T., and Risteski, A. Iterative feature matching: Toward provable domain generalization with logarithmic environments. *arXiv preprint arXiv:2106.09913*, 2021.
- Daleckii, J. L. and Krein, S. Integration and differentiation of functions of hermitian operators and applications to the theory of perturbations. *AMS Translations (2)*, 47(1-30), 1965.
- Deshmukh, A. A., Lei, Y., Sharma, S., Dogan, Ü., Cutler, J. W., and Scott, C. D. A generalization error bound for multi-class domain generalization. *ArXiv*, abs/1905.10392, 2019.
- Fang, C., Xu, Y., and Rockmore, D. N. Unbiased metric learning: On the utilization of multiple datasets and web images for softening bias. In *2013 IEEE International Conference on Computer Vision*, pp. 1657–1664, 2013. doi: 10.1109/ICCV.2013.208.
- Ganin, Y., Ustinova, E., Ajakan, H., Germain, P., Larochelle, H., Laviolette, F., Marchand, M., and Lempitsky, V. Domain-adversarial training of neural networks. *J. Mach. Learn. Res.*, 17(1):2096–2030, jan 2016. ISSN 1532-4435.
- Geirhos, R., Rubisch, P., Michaelis, C., Bethge, M., Wichmann, F. A., and Brendel, W. Imagenet-trained CNNs are biased towards texture; increasing shape bias improves accuracy and robustness. In *International Conference on Learning Representations*, 2019.
- Goodfellow, I. J., Bengio, Y., and Courville, A. *Deep Learning*. MIT Press, Cambridge, MA, USA, 2016. <http://www.deeplearningbook.org>.
- Gulrajani, I. and Lopez-Paz, D. In search of lost domain generalization. In *International Conference on Learning Representations*, 2021.
- He, K., Zhang, X., Ren, S., and Sun, J. Deep residual learning for image recognition. In *2016 IEEE Conference on Computer Vision and Pattern Recognition (CVPR)*, pp. 770–778, 2016. doi: 10.1109/CVPR.2016.90.
- Heagerty, P. J. and Zeger, S. L. Marginalized multilevel models and likelihood inference (with comments and a rejoinder by the authors). *Statistical Science*, 15(1):1 – 26, 2000. doi: 10.1214/ss/1009212671.
- Idrissi, B. Y., Arjovsky, M., Pezeshki, M., and Lopez-Paz, D. Simple data balancing achieves competitive worst-group-accuracy. *arXiv preprint arXiv:2110.14503*, 2021.
- Kamath, P., Tangella, A., Sutherland, D., and Srebro, N. Does invariant risk minimization capture invariance? In Banerjee, A. and Fukumizu, K. (eds.), *Proceedings of The 24th International Conference on Artificial Intelligence and Statistics*, volume 130 of *Proceedings of Machine Learning Research*, pp. 4069–4077. PMLR, 13–15 Apr 2021.
- Kaushik, D. and Lipton, Z. C. How much reading does reading comprehension require? a critical investigation of popular benchmarks. In *EMNLP*, pp. 5010–5015, 2018.
- Kereta, Z. and Klock, T. Estimating covariance and precision matrices along subspaces. *Electronic Journal of Statistics*, 15:554–588, 01 2021. doi: 10.1214/20-EJS1782.
- Kingma, D. P. and Ba, J. Adam: A method for stochastic optimization. In Bengio, Y. and LeCun, Y. (eds.), *3rd International Conference on Learning Representations*,

- ICLR 2015, San Diego, CA, USA, May 7-9, 2015, Conference Track Proceedings*, 2015.
- Koltchinskii, V. and Lounici, K. Concentration inequalities and moment bounds for sample covariance operators. *Bernoulli*, 23(1):110 – 133, 2017. doi: 10.3150/15-BEJ730.
- LeCun, Y., Bengio, Y., and Hinton, G. Deep learning. *Nature*, 521(7553):436–444, May 2015. ISSN 1476-4687. doi: 10.1038/nature14539.
- Li, D., Yang, Y., Song, Y., and Hospedales, T. M. Deeper, broader and artier domain generalization. In *2017 IEEE International Conference on Computer Vision (ICCV)*, pp. 5543–5551, Los Alamitos, CA, USA, oct 2017. IEEE Computer Society. doi: 10.1109/ICCV.2017.591.
- Li, K.-C. and Duan, N. Regression Analysis Under Link Violation. *The Annals of Statistics*, 17(3):1009 – 1052, 1989. doi: 10.1214/aos/1176347254.
- Li, Y., Wang, N., Shi, J., Liu, J., and Hou, X. Revisiting batch normalization for practical domain adaptation. *Pattern Recognition*, 80, 03 2016. doi: 10.1016/j.patcog.2018.03.005.
- Liu, D. C. and Nocedal, J. On the limited memory bfgs method for large scale optimization. *Mathematical Programming*, 45(1):503–528, Aug 1989. ISSN 1436-4646. doi: 10.1007/BF01589116.
- Miller, J., Krauth, K., Recht, B., and Schmidt, L. The effect of natural distribution shift on question answering models. In III, H. D. and Singh, A. (eds.), *Proceedings of the 37th International Conference on Machine Learning*, volume 119 of *Proceedings of Machine Learning Research*, pp. 6905–6916. PMLR, 13–18 Jul 2020.
- Muandet, K., Balduzzi, D., and Schölkopf, B. Domain generalization via invariant feature representation. In Dasgupta, S. and McAllester, D. (eds.), *Proceedings of the 30th International Conference on Machine Learning*, volume 28 of *Proceedings of Machine Learning Research*, pp. 10–18, Atlanta, Georgia, USA, 17–19 Jun 2013. PMLR.
- Peng, X., Bai, Q., Xia, X., Huang, Z., Saenko, K., and Wang, B. Moment matching for multi-source domain adaptation. In *Proceedings of the IEEE International Conference on Computer Vision*, pp. 1406–1415, 2019.
- Peters, J., Bühlmann, P., and Meinshausen, N. Causal inference by using invariant prediction: identification and confidence intervals. *Journal of the Royal Statistical Society*, 2016.
- Poliak, A., Naradowsky, J., Haldar, A., Rudinger, R., and Van Durme, B. Hypothesis only baselines in natural language inference. In *Proceedings of the Seventh Joint Conference on Lexical and Computational Semantics*, pp. 180–191, New Orleans, Louisiana, June 2018. Association for Computational Linguistics. doi: 10.18653/v1/S18-2023.
- Recht, B., Roelofs, R., Schmidt, L., and Shankar, V. Do ImageNet classifiers generalize to ImageNet? In Chaudhuri, K. and Salakhutdinov, R. (eds.), *Proceedings of the 36th International Conference on Machine Learning*, volume 97 of *Proceedings of Machine Learning Research*, pp. 5389–5400. PMLR, 09–15 Jun 2019.
- Rojas-Carulla, M., Schölkopf, B., Turner, R., and Peters, J. Invariant models for causal transfer learning. *J. Mach. Learn. Res.*, 19(1):1309–1342, jan 2018. ISSN 1532-4435.
- Rosenfeld, E., Ravikumar, P., and Risteski, A. The risks of invariant risk minimization. In *International Conference on Learning Representations*, 2021.
- Rosenfeld, E., Ravikumar, P., and Risteski, A. An online learning approach to interpolation and extrapolation in domain generalization. In *Proceedings of The 25th International Conference on Artificial Intelligence and Statistics*, Proceedings of Machine Learning Research. PMLR, 2022.
- Rothenhäusler, D., Meinshausen, N., Bühlmann, P., and Peters, J. Anchor regression: Heterogeneous data meet causality. *Journal of the Royal Statistical Society Series B*, 83(2):215–246, 2021.
- Sagawa, S., Koh, P. W., Hashimoto, T. B., and Liang, P. Distributionally robust neural networks. In *International Conference on Learning Representations*, 2020.
- Segù, M., Tonioni, A., and Tombari, F. Batch normalization embeddings for deep domain generalization. *arXiv preprint arXiv:2011.12672*, 2020.
- Seo, S., Suh, Y., Kim, D., Kim, G., Han, J., and Han, B. Learning to optimize domain specific normalization for domain generalization. *arXiv preprint arXiv:1907.04275*, 2019.
- Stojanov, P., Li, Z., Gong, M., Cai, R., Carbonell, J. G., and Zhang, K. Domain adaptation with invariant representation learning: What transformations to learn? In Beygelzimer, A., Dauphin, Y., Liang, P., and Vaughan, J. W. (eds.), *Advances in Neural Information Processing Systems*, 2021.

- Sun, B. and Saenko, K. Deep coral: Correlation alignment for deep domain adaptation. In Hua, G. and Jégou, H. (eds.), *Computer Vision – ECCV 2016 Workshops*, pp. 443–450, Cham, 2016. Springer International Publishing. ISBN 978-3-319-49409-8.
- Sun, Y., Wang, X., Zhuang, L., Miller, J., Hardt, M., and Efros, A. A. Test-time training with self-supervision for generalization under distribution shifts. In *ICML*, 2020.
- Vapnik, V. An overview of statistical learning theory. *IEEE Transactions on Neural Networks*, 10(5):988–999, 1999. doi: 10.1109/72.788640.
- Venkateswara, H., Eusebio, J., Chakraborty, S., and Panchanathan, S. Deep hashing network for unsupervised domain adaptation. *2017 IEEE Conference on Computer Vision and Pattern Recognition (CVPR)*, pp. 5385–5394, 2017.
- Wald, Y., Feder, A., Greenfeld, D., and Shalit, U. On calibration and out-of-domain generalization. In Beygelzimer, A., Dauphin, Y., Liang, P., and Vaughan, J. W. (eds.), *Advances in Neural Information Processing Systems*, 2021.
- Xiao, K. Y., Engstrom, L., Ilyas, A., and Madry, A. Noise or signal: The role of image backgrounds in object recognition. In *International Conference on Learning Representations*, 2021.
- Yu, Y., Wang, T., and Samworth, R. J. A useful variant of the Davis–Kahan theorem for statisticians. *Biometrika*, 102(2):315–323, 04 2014. ISSN 0006-3444. doi: 10.1093/biomet/asv008.
- Zhao, H., Combes, R. T. D., Zhang, K., and Gordon, G. On learning invariant representations for domain adaptation. In Chaudhuri, K. and Salakhutdinov, R. (eds.), *Proceedings of the 36th International Conference on Machine Learning*, volume 97 of *Proceedings of Machine Learning Research*, pp. 7523–7532. PMLR, 09–15 Jun 2019.

A. Discussion

A.1. Connection to Anchor Regression

The idea of adjusting for domain projections has similarities to Anchor Regression (Rothenhäusler et al., 2021), an objective which linearly regresses separately on the projection and rejection of the data onto the span of a set of *anchor variables*. These variables represent some (known) measure of variability across the data, and the resulting solution enjoys robustness to pointwise-additive shifts in the underlying SCM. If we define the anchor variable to be a one-hot vector indicating a sample’s environment, the Anchor Regression objective minimizes

$$\frac{1}{|\mathcal{E}|} \sum_{e \in \mathcal{E}} \mathbb{E}_{p^e} [\ell(\beta^T(x - \mu_e), y - \mu_{y,e}) + \gamma \ell(\beta^T \mu_e, \mu_{y,e})],$$

where ℓ is the squared loss and $\mu_{y,e} = \mathbb{E}_{p^e}[y]$. Here we see that Anchor Regression is “adjusting” in a sense, by regressing on the residuals, though the objective also regresses the mean prediction onto the target mean. Unfortunately, this requires access to the target mean, which is unavailable in logistic regression due to the lack of a good estimator for $\mathbb{E} \left[\log \frac{p(y=1|x)}{p(y=-1|x)} \right]$. Nevertheless, if we (i) assume the feature covariance is fixed for all environments, (ii) assume the target mean is zero for all environments, and (iii) take $\gamma \rightarrow \infty$, we observe that the above objective becomes equivalent to DARE for linear regression (2). Alternatively, we could imagine combining the two by keeping Anchor Regression’s use of separate target means while adding DARE’s feature covariance whitening which would give

$$\frac{1}{|\mathcal{E}|} \sum_{e \in \mathcal{E}} \mathbb{E}_{p^e} \left[\ell(\beta^T \Sigma_e^{-1/2}(x - \mu_e), y - \mu_{y,e}) + \gamma \ell(\beta^T \Sigma_e^{-1/2} \mu_e, \mu_{y,e}) \right],$$

However, this still requires us to estimate the target mean, so it is unclear if or how this objective could be applied to the task of classification.

B. Proofs of Main Results

B.1. Notation

We use capital letters to denote matrices and lowercase to denote vectors or scalars, where the latter should be clear from context. $\|\cdot\|$ refers to the usual vector norm, or spectral norm for matrices. For a matrix M , we use $\lambda_{\max}(M)$ to mean its maximum eigenvalue—the minimum is defined analogously. We write the pseudo-inverse as M^\dagger . For a collection of samples $\{x_i\}_{i=1}^n$, we frequently make use of the sample mean, $\hat{\mu} := \frac{1}{n} \sum x_i$, and the sample covariance, $\hat{\Sigma} := \frac{1}{n} \sum (x_i - \bar{\mu})(x_i - \bar{\mu})^T$. The notation \lesssim means less than or equal to up to constant factors.

B.2. Statement and proof of Lemma B.1, and discussion of related results

Lemma B.1. Assume our data follows a logistic regression model with regression vector β^* and covariates $z \sim \mathcal{N}(0, I)$: $\log \frac{p(y=1|z)}{p(y=-1|z)} = \beta^{*T} z$. Then the solution to the dimension-constrained logistic regression problem

$$\arg \min_{\beta} \mathbb{E}_{z,y} [-\log \sigma(y\beta^T z)] \quad \text{s.t. } \beta_{S^c} = \mathbf{0},$$

where $S \subseteq [d]$ indexes a subset of the dimensions, is equal to $\alpha \beta_S^*$ for some $\alpha \in (0, 1]$.

Proof. The logistic regression model can be rewritten:

$$y \mid z = \mathbf{1}\{\beta^{*T} z + \epsilon > 0\},$$

where ϵ is drawn from a standard logistic distribution. If we are restricted to not use z_{S^c} , we can see that these can be modeled simply as an additional noise term. Thus, our new model is

$$y \mid z = \mathbf{1}\{\beta_S^{*T} z_S + \epsilon + \tau > 0\},$$

where $\tau := \beta_{S^c}^{*T} z_{S^c} \sim p$ is symmetric zero-mean noise, independent of z_S . Because we are now modeling the other dimensions as noise, moving forward we will drop the S subscript, writing simply $\beta^{*T} z$. Define F, f as the CDF and PDF of the distribution of $\epsilon' := \epsilon + \tau$. Then the MLE population objective can be written

$$\mathcal{L}(\beta) = -\mathbb{E}_z[\mathbb{E}_{\epsilon' \sim f(\epsilon')}[\mathbf{1}\{\beta^{*T} z + \epsilon' > 0\} \log \sigma(\beta^T z) + \mathbf{1}\{-(\beta^{*T} z + \epsilon') > 0\} \log \sigma(-\beta^T z)]].$$

For a fixed z , note that $\mathbb{E}_{\epsilon'}[\mathbf{1}\{\beta^{*T} z + \epsilon' > 0\}] = \mathbb{P}(\epsilon' \geq -\beta^{*T} z) = F(\beta^{*T} z)$ (since f is symmetric), and therefore taking the derivative of this objective we get

$$\begin{aligned} \nabla_\beta \mathcal{L}(\beta) &= -\nabla_\beta \mathbb{E}_z[F(\beta^{*T} z) \log \sigma(\beta^T z) + F(-\beta^{*T} z) \log \sigma(-\beta^T z)] \\ &= \mathbb{E}_z[z \cdot (F(-\beta^{*T} z) \sigma(\beta^T z) - F(\beta^{*T} z) \sigma(-\beta^T z))] \end{aligned}$$

Because f is symmetric, we have $F(z) = 1 - F(-z)$, giving

$$\nabla_\beta \mathcal{L}(\beta) = \mathbb{E}_z[z \cdot (\sigma(\beta^T z) - F(\beta^{*T} z))].$$

Consider the directional derivative of the loss in the direction β^* , at the point $\beta = \alpha\beta^*$:

$$\beta^{*T} \nabla_\beta \mathcal{L}(\alpha\beta^*) = \mathbb{E}_z[\beta^{*T} z \cdot (\sigma(\alpha\beta^{*T} z) - F(\beta^{*T} z))].$$

Because F is the CDF of a logistic distribution convolved with p , by Fubini's theorem we have

$$\begin{aligned} F(z) &= \int_{-\infty}^z f(z) dz \\ &= \int_{-\infty}^z \left[\int_{-\infty}^{\infty} p(\tau) \sigma'(z - \tau) d\tau \right] dz \\ &= \int_{-\infty}^{\infty} p(\tau) \left[\int_{-\infty}^{z-\tau} \sigma'(\omega) d\omega \right] d\tau \\ &= \int_{-\infty}^{\infty} p(\tau) \sigma(z - \tau) d\tau \\ &= \mathbb{E}_{\tau \sim p}[\sigma(z - \tau)]. \end{aligned}$$

Further, because p is symmetric, this is equal to $\frac{1}{2} (\mathbb{E}_{\tau \sim p}[\sigma(z - \tau)] + \mathbb{E}_{\tau \sim p}[\sigma(z + \tau)])$. Thus, we have

$$\beta^{*T} \nabla_\beta \mathcal{L}(\alpha\beta^*) = \mathbb{E}_z \left[\beta^{*T} z \cdot \mathbb{E}_{\tau \sim p} \left[\sigma(\alpha\beta^{*T} z) - \frac{1}{2} (\sigma(\beta^{*T} z - \tau) + \sigma(\beta^{*T} z + \tau)) \right] \right].$$

We first consider the case where $\alpha = 1$. When $\beta^{*T} z > 0$, the term inside the expectation is positive for all $\tau \neq 0$, and vice-versa when $\beta^{*T} z < 0$ (this can be verified by writing the difference as a function of $\beta^{*T} z, \tau$, and observing that all the terms are non-negative except for a factor of $e^{\beta^{*T} z} - 1$). It follows that at the point $\beta = \beta^*$, $-\beta^*$ is a descent direction. Furthermore, since the objective is continuous in α , we can follow this direction by reducing α (that is, moving in the direction $-\beta^*$) until the directional derivative vanishes.

Next, consider $\alpha = 0$. Then the directional derivative is

$$\beta^{*T} \nabla_\beta \mathcal{L}(0) = \frac{1}{2} \mathbb{E}_z [\beta^{*T} z \cdot \mathbb{E}_{\tau \sim p} [1 - (\sigma(\beta^{*T} z - \tau) + \sigma(\beta^{*T} z + \tau))]].$$

Here, when $\beta^{*T} z > 0$ the inner term is negative, and vice-versa for $\beta^{*T} z < 0$, implying that the directional derivative is now negative. Because the objective is convex, it follows that the optimal choice for α lies in $(0, 1]$, being equal to 1 when $\tau = 0$ almost surely.

It remains to show that the optimal vector has no other component orthogonal to β^* —in other words, that the solution is precisely $\alpha\beta^*$. For isotropic Gaussian z , we have for any δ perpendicular to β^* that $\mathbb{E}[\delta^T z | \beta^{*T} z] = 0$. Therefore, the gradient in the direction δ is

$$\begin{aligned} \mathbb{E}_z[\delta^T z \cdot (\sigma(\alpha\beta^{*T} z) - F(\beta^{*T} z))] &= \mathbb{E}_{\beta^{*T} z}[\mathbb{E}_{\delta^T z | \beta^{*T} z}[\delta^T z] (\sigma(\alpha\beta^{*T} z) - F(\beta^{*T} z))] \\ &= 0. \end{aligned}$$

Since β^* and all orthogonal directions form a complete basis, it follows that $\nabla \mathcal{L}(\alpha\beta^*) = 0$ and therefore that $\alpha\beta^*$ is the optimal solution. \square

Though we prove this lemma only for Gaussian z , we found empirically that the result approximately holds whenever z is dimension-wise independent and symmetric about the origin. We believe this is a consequence of the Central Limit Theorem: our proof relies on the conditional expectation of inner products with z which converge to Gaussian in distribution as the dimensionality of z grows.

We observe that Li & Duan (1989) prove a much simpler result under a general “linear conditional expectation” condition which is similar to the property we exploit regarding zero-mean conditional expectation of orthogonal inner products with isotropic Gaussians. Their result is more general, but it allows for any value of α , including negative. In this case, we would actually be recovering the *opposite* effects of the ground truth, which is clearly insufficient for test-time prediction. Heagerty & Zeger (2000) give an analytical closed-form for the solution under a probit model with Gaussian noise; since this is not a logistic model, the Gaussian noise represents significantly less model mis-specification, which explains why the exact closed-form is recoverable.

B.3. Proof of Theorem 5.2

Theorem 5.2. (Closed-form solution to the DARE population objective). *Under model (3), the solution to the DARE population objective (2) for linear regression is $\hat{\Pi}\beta^*$. If ϵ is Gaussian, then the solution for logistic regression (1) is $\alpha\hat{\Pi}\beta^*$ for some $\alpha \in (0, 1]$.*

Proof. Observe that under the constraint, regressing on the centered observations is equivalent to regressing on the non-centered observations (since the mean must have no effect on the output), so the solutions to these two objectives must be the same and have the same minimizers. We therefore consider the solution to the DARE objective but on non-centered observations.

It is immediate that the unconstrained solution to the DARE population objective on non-centered data is β^* for both linear and logistic regression. For linear regression, we observe that because the adjusted covariates in each environment have identity covariance, the excess training risk of a predictor β is exactly $\|\beta - \beta^*\|^2$. Therefore, the solution can be rewritten

$$\begin{aligned} \min_{\beta} \quad & \|\beta - \beta^*\|^2 \\ \text{s.t.} \quad & \beta^T \Sigma_e^{-1/2} \mu_e = 0. \quad \forall e \in \mathcal{E}. \end{aligned}$$

Recalling that $\Sigma_e^{-1/2} \mu_e = b_e$, the constraint can be written in matrix form as $\mathbb{B}^T \beta = \mathbf{0}$, and thus we see that the solution is the ℓ_2 -norm projection of β^* onto the nullspace of \mathbb{B}^T (i.e., the intersection of the nullspaces of the b_e). By definition, this is given by $(I - \mathbb{B}\mathbb{B}^\dagger)\beta^* = \hat{\Pi}\beta^*$.

To derive the closed-form for logistic regression, write the spectral decomposition $\mathbb{B} = UDV^T$, and consider regressing on $U^T \epsilon$ instead of ϵ . As the predictor only affects the objective through its linear projection, the solution to this objective will be U^T times the solution to the original objective (that is, for all vectors v , $(U^T \beta)^T U^T v = \beta^T v$). We will denote parameters for the rotated objective with a tilde, e.g. $\tilde{v} := U^T v$.

The constraint in (1) is equivalent to requiring that the mean projection is a constant vector $c\mathbf{1}$ and, with the inclusion of a bias term, we can WLOG consider $c = 0$. Thus, the constraint can be written $\mathbb{B}^T \tilde{\beta} = VD\tilde{\beta} = \mathbf{0} \iff D\tilde{\beta} = \mathbf{0}$. We can therefore see that this constraint is the same as requiring that the dimensions of $\tilde{\beta}$ corresponding to the non-zero dimensions of D are 0.

Noting that $U^T \epsilon \sim \mathcal{N}(0, I)$, we now apply Lemma B.1 to see that the solution will be $\tilde{\beta} = \alpha(I - DD^\dagger)\tilde{\beta}^*$ for some $\alpha \in (0, 1]$. Finally, as argued above we can recover the solution to the original objective by rotating back, giving the solution $\beta = U\tilde{\beta} = \alpha U(I - DD^\dagger)U^T \beta^* = \alpha\hat{\Pi}\beta^*$. \square

B.4. Proof of Theorem 5.7

Theorem B.2 (Theorem 5.7, restated). *For any $\rho \geq 0$, denote the set of possible test environments \mathcal{A}_ρ which contains all parameters $(A_{e'}, b_{e'})$ subject to Assumptions 5.4 and 5.6 and a bound on the mean: $\|b_{e'}\| \leq \rho$. For logistic or linear regression, let $\hat{\beta}$ be the minimizer of the corresponding DARE objective (1) or (2). Then,*

$$\sup_{(A_{e'}, b_{e'}) \in \mathcal{A}_\rho} \mathcal{R}_{e'}(\hat{\beta}) = (1 + \rho^2)(\|\beta^*\|^2 + 2B\|\beta_{\hat{\Pi}}^*\|\|\beta_{I-\hat{\Pi}}^*\|).$$

Furthermore, the DARE solution is minimax:

$$\hat{\beta} \in \arg \min_{\beta \in \mathbb{R}^d} \sup_{(A_{e'}, b_{e'}) \in \mathcal{A}_\rho} \mathcal{R}_{e'}(\beta).$$

Proof. Recall that in an environment e , $\mathbb{E}_e[y | x] = \beta^{*T} \Sigma_e^{-1/2} x$. So, for an environment e' and predictor $\hat{\beta}$, we have the following excess risk decomposition:

$$\begin{aligned} \mathcal{R}_{e'}(\hat{\beta}) &= \mathbb{E}_{e'}[(\hat{\beta}^T \bar{\Sigma}^{-1/2} x' - \beta^{*T} \Sigma_{e'}^{-1/2} x')^2] \\ &= \underbrace{\mathbb{E}_{e'}[(\hat{\beta}^T \bar{\Sigma}^{-1/2} (x' - \mu_{e'}) - \beta^{*T} \Sigma_{e'}^{-1/2} (x' - \mu_{e'}))^2]}_{T_1} + \underbrace{\mathbb{E}_{e'}[(\hat{\beta}^T \bar{\Sigma}^{-1/2} \mu_{e'} - \beta^{*T} \Sigma_{e'}^{-1/2} \mu_{e'})^2]}_{T_2}. \end{aligned}$$

Observe that term T_1 does not depend on the mean $b_{e'}$.

Term T_2 simplifies to

$$\mathbb{E}_{e'}[(\hat{\beta}^T \bar{\Sigma}^{-1/2} \mu_{e'} - \beta^{*T} \Sigma_{e'}^{-1/2} \mu_{e'})^2] = \left(\overbrace{(\Sigma_{e'}^{1/2} \bar{\Sigma}^{-1/2} \hat{\beta} - \beta^*)^T}^v b_{e'} \right)^2,$$

and so we can write a supremum over T_2 as

$$\begin{aligned} \sup_{\mathcal{A}_\rho} T_2 &= \sup_{\mathcal{A}_\rho} (v^T b_{e'})^2 \\ &= \rho^2 \sup_{\mathcal{A}_\rho} \|v\|^2. \end{aligned}$$

Next, observe that T_1 simplifies to

$$\begin{aligned} \hat{\beta}^T \bar{\Sigma}^{-1/2} \Sigma_{e'} \bar{\Sigma}^{-1/2} \hat{\beta} + \|\beta^*\|^2 - 2\hat{\beta}^T \bar{\Sigma}^{-1/2} \Sigma_{e'}^{1/2} \beta^* &= \|\Sigma_{e'}^{1/2} \bar{\Sigma}^{-1/2} \hat{\beta} - \beta^*\|^2 \\ &= \|v\|^2. \end{aligned}$$

So, returning to the full loss and recalling that T_1 is independent of $b_{e'}$, we have

$$\begin{aligned} \sup_{\mathcal{A}_\rho} \mathcal{R}_{e'}(\hat{\beta}) &= \sup_{\mathcal{A}_\rho} T_1 + T_2 \\ &= (1 + \rho^2) \sup_{\mathcal{A}_\rho} \|v\|^2. \end{aligned}$$

Of course, the ideal would be for a given environment e' to set $\hat{\beta} := \bar{\Sigma}^{1/2} \Sigma_{e'}^{-1/2} \beta^* \implies v = 0$, but we have to choose a single $\hat{\beta}$ for all possible environments e' parameterized by $(A_{e'}, b_{e'}) \in \mathcal{A}_\rho$. We will show that the choice of $\hat{\beta} := \alpha \hat{\Pi} \beta^*$ is minimax-optimal under this set for any $\alpha \in (0, 1]$.

Leaving the supremum over adversary choices implicit, we can rewrite the squared norm of v as

$$\begin{aligned} v^T v &= ((\Delta + I) \hat{\beta} - \beta^*)^T ((\Delta + I) \hat{\beta} - \beta^*) \\ &= \hat{\beta}^T \Delta^T \Delta \hat{\beta} + \|\hat{\beta} - \beta^*\|^2 + 2\hat{\beta}^T \Delta^T (\hat{\beta} - \beta^*). \end{aligned}$$

By Lemma C.4, we can define an environment by defining the block terms of $U_{\hat{\Pi}} \Delta U_{\hat{\Pi}}^T$ directly. Consider the choice of $\Delta_1 = \lambda \frac{\hat{\beta}_{I-\hat{\Pi}} \hat{\beta}_{I-\hat{\Pi}}^T}{\|\hat{\beta}_{I-\hat{\Pi}}\|^2}$, $\Delta_2 = \Delta_{12} = \Delta_{21} = \mathbf{0}$. This choice is in \mathcal{A}_ρ for any $\lambda \in \mathbb{R}$ since it is block-diagonal and $\|\Delta_2\| = 0$. Now we can write

$$\begin{aligned} v^T v &= \lambda^2 \|\hat{\beta}_{I-\hat{\Pi}}\|^2 + \|\hat{\beta} - \beta^*\|^2 + 2\lambda \hat{\beta}_{I-\hat{\Pi}}^T (\hat{\beta}_{I-\hat{\Pi}} - \beta_{I-\hat{\Pi}}^*) \\ &\geq \lambda^2 \|\hat{\beta}_{I-\hat{\Pi}}\|^2 - 2\lambda \|\hat{\beta}_{I-\hat{\Pi}}\| \|\hat{\beta} - \beta^*\|, \end{aligned}$$

via Cauchy-Schwarz and the triangle inequality. So, taking $\lambda \rightarrow \infty$ means that the minimax risk is unbounded unless $\hat{\beta}_{I-\hat{\Pi}} = 0 \iff \hat{\beta} = \hat{\beta}_{\hat{\Pi}}$. For the remainder of the proof we consider only this case.

With this restriction, we have

$$\begin{aligned} \|v\|^2 &= \|(\Delta + I)\hat{\beta}_{\hat{\Pi}} - \beta^*\|^2 \\ &= \|(\Delta + I)\hat{\beta}_{\hat{\Pi}} - \beta_{\hat{\Pi}}^* - \beta_{I-\hat{\Pi}}^*\|^2 \\ &= \|(\Delta + I)\hat{\beta}_{\hat{\Pi}} - \beta_{\hat{\Pi}}^*\|^2 + \|\beta_{I-\hat{\Pi}}^*\|^2 - 2\beta_{I-\hat{\Pi}}^{*T}\Delta\hat{\beta}_{\hat{\Pi}}. \end{aligned}$$

Assumption 5.4 implies that

$$\begin{aligned} |\beta_{I-\hat{\Pi}}^{*T}\Delta\hat{\beta}_{\hat{\Pi}}| &= |\beta^{*T}U_{\hat{\Pi}}(I - S_{\hat{\Pi}})U_{\hat{\Pi}}^T\Delta U_{\hat{\Pi}}S_{\hat{\Pi}}U_{\hat{\Pi}}^T\hat{\beta}| \\ &= \left| \beta^{*T}U_{\hat{\Pi}}(I - S_{\hat{\Pi}}) \begin{bmatrix} \Delta_1 & \Delta_{12} \\ \Delta_{21} & \Delta_2 \end{bmatrix} S_{\hat{\Pi}}U_{\hat{\Pi}}^T\hat{\beta} \right| \\ &\leq B\|\beta_{\hat{\Pi}}^*\|\|\beta_{I-\hat{\Pi}}^*\|, \end{aligned}$$

Consider the DARE solution $\hat{\beta} = \alpha\beta_{\hat{\Pi}}^*$ for $\alpha \in (0, 1]$. Then using the equivalent supremized set from Assumption 5.6 and Lemma C.3, the worst-case risk of this choice is

$$\begin{aligned} \sup_{\mathcal{A}_\rho} \mathcal{R}_{e'}(\hat{\beta}) &= (1 + \rho^2) \sup_{\|\Delta\beta_{\hat{\Pi}}^*\|^2 < \|\beta_{\hat{\Pi}}^*\|^2} (\|(\alpha\Delta + (\alpha - 1)I)\beta_{\hat{\Pi}}^*\|^2 + \|\beta_{I-\hat{\Pi}}^*\|^2 + 2B\|\beta_{\hat{\Pi}}^*\|\|\beta_{I-\hat{\Pi}}^*\|) \\ &= (1 + \rho^2)(\|\beta_{\hat{\Pi}}^*\|^2 + \|\beta_{I-\hat{\Pi}}^*\|^2 + 2B\|\beta_{\hat{\Pi}}^*\|\|\beta_{I-\hat{\Pi}}^*\|). \end{aligned} \quad (4)$$

It remains to show that any other choice of $\hat{\beta}$ results in greater risk. Observe that the second two terms of (4) are constant with respect to Δ , so we focus on the first term. That is, we show that any other choice results in $\sup_{\|\Delta\beta_{\hat{\Pi}}^*\|^2 < \|\beta_{\hat{\Pi}}^*\|^2} \|(\Delta + I)\hat{\beta}_{\hat{\Pi}} - \beta_{\hat{\Pi}}^*\|^2 > \|\beta_{\hat{\Pi}}^*\|^2$ (except for $\hat{\beta} = 0$, which we address at the end).

For any choice of $\hat{\beta}_{\hat{\Pi}}$, decompose the vector into its projection and rejection onto $\beta_{\hat{\Pi}}^*$ as $\hat{\beta}_{\hat{\Pi}} = \alpha\beta_{\hat{\Pi}}^* + \delta$, with $\delta^T\beta_{\hat{\Pi}}^* = 0$. The adversary can choose $\Delta_2 = \lambda\delta\delta^T$, which lies in \mathcal{A}_ρ for any λ . Then taking $\lambda \rightarrow \infty$ causes risk to grow without bound—it follows that we must have $\delta = 0$.

Next, consider any choice $\alpha \notin (0, 1]$. If $\alpha > 2$ or $\alpha < 0$, choosing $\Delta_2 = 0$ makes this term $(\alpha - 1)^2\|\beta_{\hat{\Pi}}^*\|^2 > \|\beta_{\hat{\Pi}}^*\|^2$. If $2 \geq \alpha > 1$, choosing $\Delta_2 = \frac{1}{\alpha}I$ makes this term $\alpha^2\|\beta_{\hat{\Pi}}^*\|^2 > \|\beta_{\hat{\Pi}}^*\|^2$.

Finally, if $\alpha = 0$ then this term is equal to $\|\beta_{\hat{\Pi}}^*\|^2$ —however, this value is the *supremum* of the adversarial risk of the DARE solution and it cannot actually be attained. \square

B.5. Proof of Theorem 5.10

Theorem B.3 (Theorem 5.10, restated). *Fix test environment parameters $A_{e'}, b_{e'}$ and our guess $\bar{\Sigma}$. Suppose we minimize the DARE regression objective (2) on environments whose means b_e are Gaussian vectors with covariance Σ_b , with $\text{span}(\Sigma_b) = \text{span}(I - \Pi)$. After seeing E training domains:*

1. *If $E \geq \text{rank}(\Sigma_b)$ then DARE recovers the minimax-optimal predictor almost surely: $\hat{\beta} = \beta_{\Pi}^*$.*
2. *Otherwise, if $E \geq r(\Sigma_b)$ then with probability $\geq 1 - \delta$,*

$$\mathcal{R}_{e'}(\hat{\beta}) \leq \mathcal{R}_{e'}(\beta_{\Pi}^*) + \mathcal{O}\left(\frac{\|\Sigma_b\|}{\xi(\Sigma_b)} \left(\sqrt{\frac{r(\Sigma_b)}{E}} + \max\left\{ \sqrt{\frac{\log 1/\delta}{E}}, \frac{\log 1/\delta}{E} \right\} \right)\right),$$

where $\mathcal{O}(\cdot)$ hides dependence on $\|\Delta\|$.

Proof. Define $\hat{\Pi}_E$ as the projection onto the nullspace of \mathbb{B}^T after having seen E environments. Item 1 is immediate, since as soon as we observe $E = \text{rank}(\Sigma_b)$ linearly independent b_e we have that $\text{span}(\mathbb{B}) = \text{span}(\Sigma_b)$ and therefore $\hat{\Pi}_E = \Pi$

(this occurs almost surely for any absolutely continuous distribution). To prove item 2, we will write the solution learned after seeing E environments as $\hat{\beta}_E := \hat{\Pi}_E \beta^*$. We can write the excess risk of the ground-truth minimax predictor β_Π^* as

$$\begin{aligned}\mathcal{R}_{e'}(\beta_\Pi^*) &= \mathbb{E}[(\beta_\Pi^{*T} \bar{\Sigma}^{-1/2} \Sigma_{e'}^{1/2} \epsilon - \beta^{*T} \epsilon)^2] \\ &= \mathbb{E}[(\beta^{*T} \Pi \bar{\Sigma}^{-1/2} \Sigma_{e'}^{1/2} \epsilon - \beta^{*T} \epsilon)^2],\end{aligned}$$

and likewise we have

$$\begin{aligned}\mathcal{R}_{e'}(\hat{\beta}_E) &= \mathbb{E}[(\hat{\beta}_E^T \bar{\Sigma}^{-1/2} \Sigma_{e'}^{1/2} \epsilon - \beta^{*T} \epsilon)^2] \\ &= \mathbb{E}[(\beta^{*T} \hat{\Pi}_E \bar{\Sigma}^{-1/2} \Sigma_{e'}^{1/2} \epsilon - \beta^{*T} \epsilon)^2].\end{aligned}$$

Taking the difference,

$$\begin{aligned}\mathcal{R}(\hat{\beta}_E) - \mathcal{R}(\beta_\Pi^*) &= \mathbb{E}[(\beta^{*T} \hat{\Pi}_E \overbrace{\bar{\Sigma}^{-1/2} \Sigma_{e'}^{1/2}}^{:=v} \epsilon - \beta^{*T} \epsilon)^2 - (\beta^{*T} \Pi \bar{\Sigma}^{-1/2} \Sigma_{e'}^{1/2} \epsilon - \beta^{*T} \epsilon)^2] \\ &\leq \|(\Pi - \hat{\Pi}_E) \mathbb{E}[vv^T](2I - \Pi - \hat{\Pi}_E)\| + 2\|(\Pi - \hat{\Pi}_E) \mathbb{E}[v\epsilon^T]\| \\ &\leq 2 \left[\|(\Pi - \hat{\Pi}_E) \mathbb{E}[vv^T]\| + \|(\Pi - \hat{\Pi}_E) \mathbb{E}[v\epsilon^T]\| \right].\end{aligned}$$

Now we note that

$$\begin{aligned}\mathbb{E}[vv^T] &= \mathbb{E}[(\bar{\Sigma}^{-1/2} \Sigma_{e'}^{1/2} \epsilon)(\bar{\Sigma}^{-1/2} \Sigma_{e'}^{1/2} \epsilon)^T] \\ &= \bar{\Sigma}^{-1/2} \Sigma_{e'} \bar{\Sigma}^{-1/2}\end{aligned}$$

and

$$\mathbb{E}[v\epsilon^T] = \bar{\Sigma}^{-1/2} \Sigma_{e'}^{1/2}.$$

These matrices are bounded by $\|\Delta + I\|^2$, $\|\Delta + I\|$ respectively and are constant with respect to the training environments we sample. It follows that we can bound the risk difference as

$$\mathcal{R}(\hat{\beta}_E) - \mathcal{R}(\beta_\Pi^*) \lesssim \|\hat{\Pi}_E - \Pi\|,$$

and all that remains is to bound the term $\|\hat{\Pi}_E - \Pi\|$.

Combining Theorems 4 and 5 from [Koltchinskii & Lounici \(2017\)](#) with the triangle inequality, we have that when $r(\Sigma_b) \leq E$, with probability $\geq 1 - \delta$,

$$\|\bar{\Sigma} - \Sigma_b\| \lesssim \|\Sigma_b\| \left(\max \left\{ \sqrt{\frac{\log 1/\delta}{E}}, \frac{\log 1/\delta}{E} \right\} + \max \left\{ \sqrt{\frac{r(\Sigma_b)}{E}}, \frac{r(\Sigma_b)}{E} \right\} \right).$$

Since $r(\Sigma_b) \leq E$, the first term of the second max dominates. Further, Corrolary 3 of [Yu et al. \(2014\)](#), a variant of the Davis-Kahan theorem, gives us

$$\|\hat{\Pi}_E - \Pi\| \lesssim \frac{\|\bar{\Sigma} - \Sigma_b\|}{\xi(\Sigma_b)}.$$

Combining these facts gives the result. \square

B.6. Proof of Theorem 5.12

Theorem B.4 (Theorem 5.12, fully stated). *Assume the data follows model (3) with $\epsilon \sim \mathcal{N}(0, I)$. Observing n_S samples from a source distribution S with covariance Σ_S , we use half to estimate $\hat{\Sigma}_S$ and the other half to learn parameters β which minimize the unconstrained ($\lambda = 0$), uncentered DARE regression objective. At test-time, given n_T samples $\{x_i\}_{i=1}^{n_T}$ from the target distribution T with mean and covariance μ_T, Σ_T , we predict $f(x; \beta) = \beta^T \hat{\Sigma}_T^{-1/2} x$.*

Define $m(\Sigma) := \frac{\lambda_{\max}(\Sigma)}{\lambda_{\min}^3(\Sigma)}$, and assume $n_S = \Omega(m(\Sigma_S)d^2)$, $n_T = \Omega(m(\Sigma_T)d^2)$. Then with probability at least $1 - 3d^{-1}$, the excess squared error of our predictor on the new environment is bounded as

$$\mathcal{R}_T(f) = \mathcal{O} \left((1 + \|\mu_T\|^2) \left(\frac{\mathbb{E}[\eta^2]}{1 - \mathcal{O}\left(\sqrt{\frac{d}{n_S}}\right)} \frac{d}{n_S} + d^2 \left(\frac{m(\Sigma_S)}{n_S} + \frac{m(\Sigma_T)}{n_T} \right) \right) \right).$$

Proof. We begin by bounding the error of our solution $\|\beta - \beta^*\|$. Observe that with our estimate $\hat{\Sigma}_S$ of the source environment moments, we are solving linear regression with targets $\beta^{*T}\epsilon_i + \eta_i$ and covariates $\hat{x}_i = \hat{\Sigma}_S^{-1/2}x_i = \hat{\Sigma}_S^{-1/2}\Sigma_S^{1/2}\epsilon_i$. Thus, if we had access to the true gradient of the modified least-squares objective (which is not the same as assuming $n_S \rightarrow \infty$, because in that case we would have $\hat{\Sigma}_S \rightarrow \Sigma_S$), the solution would be

$$\begin{aligned} \mathbb{E}[\hat{x}\hat{x}^T]^{-1}\mathbb{E}[\hat{x}y] &= \left(\hat{\Sigma}_S^{-1/2}\Sigma_S^{1/2}(I + \mu_T\mu_T^T)\Sigma_S^{1/2}\hat{\Sigma}_S^{-1/2} \right)^{-1} \left(\hat{\Sigma}_S^{-1/2}\Sigma_S^{1/2}(I + \mu_T\mu_T^T)\beta^* \right) \\ &= \hat{\Sigma}_S^{1/2}\Sigma_S^{-1/2}\beta^*. \end{aligned}$$

Moving forward we denote this solution to the modified objective as $\hat{\beta} := \hat{\Sigma}_S^{1/2}\Sigma_S^{-1/2}\beta^*$, and further define $\Delta_S := \Sigma_S^{1/2}\hat{\Sigma}_S^{-1/2}$, with Δ_T defined analogously. A classical result tells us that the OLS solution is distributed as $\mathcal{N}\left(\hat{\beta}, \frac{\sigma_y^2}{n_S}M^{-1}\right)$, where M is the modified covariance $\Delta_S^T\Delta_S$ and $\sigma_y^2 := \mathbb{E}[\eta^2]$. To show a rate of convergence to the OLS solution, we need to solve for the minimum eigenvalue $\lambda_{\min}(M)$ —this will suffice since the above fact implies finite-sample convergence of the OLS estimator to the population solution. The well-known bound for sub-Gaussian random vectors tells us that with probability $\geq 1 - \delta_1$,

$$\|\beta - \hat{\beta}\| \lesssim \sqrt{\lambda_{\max}(M^{-1})\sigma_y^2} \left(\sqrt{\frac{d}{n_S}} + \sqrt{\frac{\log 1/\delta_1}{n_S}} \right).$$

and moving forward we condition on this event. Now let $\gamma_S := \sqrt{d/n_S}$, with γ_T defined analogously. Since $M \succeq 0$, it follows that

$$\lambda_{\max}(M^{-1}) = \lambda_{\min}(\Delta_S^T\Delta_S)^{-1},$$

and further,

$$\lambda_{\min}(\Delta_S^T\Delta_S) \geq 1 - \|\Delta_S^T\Delta_S - I\|.$$

By Lemma C.1, we have that with probability $\geq 1 - d^{-1}$

$$\|\Delta_S^T\Delta_S - I\| \lesssim \gamma_S.$$

This implies that our solution's error can be bounded as

$$\begin{aligned} \|\beta - \beta^*\| &= \|(\beta - \hat{\beta}) + (\hat{\beta} - \beta^*)\| \\ &\leq \sqrt{\frac{\sigma_y^2}{1 - \mathcal{O}(\gamma_S)}} \left(\sqrt{\frac{d}{n_S}} + \sqrt{\frac{\log 1/\delta_1}{n_S}} \right) + \|\hat{\Sigma}_S^{1/2}\Sigma_S^{-1/2} - I\|\|\beta^*\| \end{aligned}$$

We assume $\|\beta^*\| = 1$ so we can avoid carrying it throughout the rest of the proof. Bounding the second term with Lemma C.2 gives

$$\|\beta - \beta^*\| \lesssim \sqrt{\frac{\sigma_y^2}{1 - \mathcal{O}(\gamma_S)}} \left(\sqrt{\frac{d}{n_S}} + \sqrt{\frac{\log 1/\delta_1}{n_S}} \right) + \gamma_S \sqrt{d m(\Sigma_S)}.$$

On the target distribution, our excess risk with a predictor β is

$$\begin{aligned}
 \mathcal{R}_{e'}(\beta) &= \mathbb{E}[(\beta^T \hat{\Sigma}_T^{-1/2} x - \beta^{*T} \Sigma_T^{-1/2} x)^2] \\
 &= \mathbb{E} \left[\left(\overbrace{(\Sigma_T^{1/2} \hat{\Sigma}_T^{-1/2})^T}^{\Delta_T} \beta - \beta^* \right)^T \epsilon \right]^2 \\
 &= (\Delta_T \beta - \beta^*)^T (I + \mu_T \mu_T^T) (\Delta_T \beta - \beta^*) \\
 &\leq (1 + \|\mu_T\|^2) \|\Delta_T \beta - \beta^*\|^2
 \end{aligned}$$

Now, we have

$$\begin{aligned}
 \|\Delta_T \beta - \beta^*\| &= \|(\Delta_T \beta - \Delta_T \beta^*) + (\Delta_T \beta^* - \beta^*)\| \\
 &\leq \|\Delta_T(\beta - \beta^*)\| + \|(\Delta_T - I)\beta^*\| \\
 &\leq (1 + \|\Delta_T - I\|) \|\beta - \beta^*\| + \|\Delta_T - I\|.
 \end{aligned}$$

Once again invoking Lemma C.2, with probability $\geq 1 - d^{-1}$,

$$\|\Delta_T - I\| \lesssim \gamma_T \sqrt{d \, m(\Sigma_T)},$$

and using this plus the previous result, the triangle inequality, and $(a + b)^2 \leq 2(a^2 + b^2)$ gives

$$\begin{aligned}
 \|\Delta_T \beta - \beta^*\|^2 &\lesssim (1 + \|\Delta_T - I\|)^2 \|\beta - \beta^*\|^2 + \|\Delta_T - I\|^2 \\
 &\lesssim (1 + \gamma_T \sqrt{d \, m(\Sigma_T)})^2 \|\beta - \beta^*\|^2 + (\|\Sigma^{1/2}\| \|\Sigma^{-1}\|^{3/2} \sqrt{d} \gamma_T)^2 \\
 &\lesssim \|\beta - \beta^*\|^2 + \gamma_T^2 d \, m(\Sigma_T),
 \end{aligned}$$

where the lower bound on n_T enforces $\gamma_T \sqrt{d \, m(\Sigma_T)} \leq 1$. It follows that the excess risk can be bounded as

$$\begin{aligned}
 \mathcal{R}_{e'} &\lesssim (1 + \|\mu_T\|^2) \|\Delta_T \beta - \beta^*\|^2 \\
 &\lesssim (1 + \|\mu_T\|^2) (\|\beta - \beta^*\|^2 + \gamma_T^2 d \, m(\Sigma_T)).
 \end{aligned}$$

Letting $\delta_1 = 1/d$, combining all of the above via union bound, and eliminating lower-order terms, we get

$$\begin{aligned}
 \mathcal{R}_{e'}(\beta) &\lesssim (1 + \|\mu_T\|^2) \left(\frac{\sigma_y^2}{1 - \mathcal{O}(\gamma_S)} \frac{d}{n_S} + \gamma_S^2 d \, m(\Sigma_S) + \gamma_T^2 d \, m(\Sigma_T) \right) \\
 &= (1 + \|\mu_T\|^2) \left(\frac{\sigma_y^2}{1 - \mathcal{O}\left(\sqrt{\frac{d}{n_S}}\right)} \frac{d}{n_S} + d^2 \left(\frac{m(\Sigma_S)}{n_S} + \frac{m(\Sigma_T)}{n_T} \right) \right)
 \end{aligned}$$

with probability $\geq 1 - 3d^{-1}$. □

C. Technical Lemmas

Lemma C.1. Suppose we observe $n \in \Omega(d + \log 1/\delta)$ samples $X \sim \mathcal{N}(\mu, \Sigma)$ with $\Sigma \succeq 0$ and estimate the inverse covariance matrix Σ^{-1} with the inverse of the sample covariance matrix $\bar{\Sigma}^{-1}$. Then with probability $\geq 1 - \delta$, it holds that

$$\|\bar{\Sigma}^{-1/2} \Sigma \bar{\Sigma}^{-1/2} - I\| \lesssim \sqrt{\frac{d + \log 1/\delta}{n}}.$$

Proof. As $\bar{\Sigma}^{-1/2} \Sigma \bar{\Sigma}^{-1/2}$ and $\Sigma^{1/2} \bar{\Sigma}^{-1} \Sigma^{1/2}$ have the same spectrum, it suffices to bound the latter. Observe that

$$\|\Sigma^{1/2} \bar{\Sigma}^{-1} \Sigma^{1/2} - I\| = \|\Sigma^{1/2} (\bar{\Sigma}^{-1} - \Sigma^{-1}) \Sigma^{1/2}\|.$$

Now applying Theorem 10 of [Kereta & Klock \(2021\)](#) with $A = B = \Sigma^{1/2}$ yields the result. \square

Lemma C.2. Assume the conditions of Lemma C.1. Then under the same event as Lemma C.1, it holds that

$$\|\Sigma^{1/2} \bar{\Sigma}^{-1/2} - I\| \lesssim \|\Sigma^{1/2}\| \left(\|\Sigma^{-1}\|^{3/2} \sqrt{d} \gamma + \|\Sigma^{-1}\|^2 \gamma^2 \right),$$

where $\gamma = \sqrt{\frac{d + \log 1/\delta}{n}}$. In particular, if $\delta = d^{-1}$, then

$$\|\Sigma^{1/2} \bar{\Sigma}^{-1/2} - I\| \lesssim \sqrt{\|\Sigma\| \|\Sigma^{-1}\|^3 \frac{d^2}{n}}$$

Proof. We begin by deriving a bound for $\|\bar{\Sigma}^{-1/2} - \Sigma^{-1/2}\|$. Define $E = \bar{\Sigma}^{-1} - \Sigma^{-1}$. Observe that

$$\begin{aligned} \|E\| &= \|\Sigma^{-1/2} \Sigma^{1/2} E \Sigma^{1/2} \Sigma^{-1/2}\| \\ &= \|\Sigma^{-1/2} (\Sigma^{1/2} \bar{\Sigma}^{-1} \Sigma^{1/2} - I) \Sigma^{-1/2}\| \\ &\leq \|\Sigma^{-1}\| \|\Sigma^{1/2} \bar{\Sigma}^{-1} \Sigma^{1/2} - I\|, \end{aligned}$$

and now apply Lemma C.1 (since $\bar{\Sigma}^{-1/2} \Sigma \bar{\Sigma}^{-1/2}$ and $\Sigma^{1/2} \bar{\Sigma}^{-1} \Sigma^{1/2}$ have the same spectrum), giving

$$\|E\| \lesssim \|\Sigma^{-1}\| \gamma.$$

Let UDU^T be the eigendecomposition of Σ , and define the matrix $[\sqrt{\cdot}, \alpha]_{i,j} = \frac{1}{\sqrt{D_{ii}} + \sqrt{D_{jj}}}$ as in [Carlsson \(2018\)](#). The Daleckii-Krein theorem ([Daleckii & Krein, 1965](#)) tells us that

$$\|\bar{\Sigma}^{-1/2} - \Sigma^{-1/2}\| = \|U([\sqrt{\cdot}, \alpha] \circ E)U^T\| + O(\|E\|^2).$$

Note that $\max_{i,j} |[\sqrt{\cdot}, \alpha]_{i,j}| = 1/2\sqrt{\lambda_{\min}(\Sigma)} \implies \|[\sqrt{\cdot}, \alpha]\| \leq \sqrt{d\|\Sigma^{-1}\|}$, and therefore by sub-multiplicativity of spectral norm under Hadamard product,

$$\begin{aligned} \|\bar{\Sigma}^{-1/2} - \Sigma^{-1/2}\| &\lesssim \sqrt{d\|\Sigma^{-1}\|} \|E\| + \|E\|^2 \\ &\lesssim \|\Sigma^{-1}\|^{3/2} \sqrt{d} \gamma + \|\Sigma^{-1}\|^2 \gamma^2. \end{aligned}$$

Finally, noting that

$$\begin{aligned} \|\Sigma^{1/2} \bar{\Sigma}^{-1/2} - I\| &= \|\Sigma^{1/2} (\bar{\Sigma}^{-1/2} - \Sigma^{-1/2})\| \\ &\leq \|\Sigma^{1/2}\| \|\bar{\Sigma}^{-1/2} - \Sigma^{-1/2}\| \end{aligned}$$

completes the main proof. To see the second claim, note that $n \geq 2\|\Sigma^{-1}\|$ implies $\|\Sigma^{-1}\|^{3/2} \sqrt{d} \geq \|\Sigma^{-1}\|^2 \gamma$, meaning the first of the two terms dominates. \square

Lemma C.3. Let $\bar{\Sigma}$ be fixed. Then Assumption 5.6 is satisfied if and only if $\|\Delta\beta_{\bar{\Sigma}}^*\|^2 < \|\beta_{\bar{\Sigma}}^*\|^2$.

Proof. The claim follows by rewriting the risk terms. Recall that $\Delta = \Sigma_{e'}^{1/2} \bar{\Sigma}^{-1/2} - I$. Writing out the excess risk of the ground truth β^* in the subspace $\hat{\Pi}$,

$$\begin{aligned} \mathcal{R}_{p_{e'}}^{\hat{\Pi}}(\beta^*) &= \mathbb{E}_{p_{e'}} \left[(\beta_{\hat{\Pi}}^{*T} \bar{\Sigma}^{-1/2} x - \beta_{\hat{\Pi}}^{*T} \Sigma_{e'}^{-1/2} x)^2 \right] \\ &= \mathbb{E}_{p_{e'}} \left[(\beta^{*T} \hat{\Pi} \bar{\Sigma}^{-1/2} \Sigma_{e'}^{1/2} \epsilon - \beta^{*T} \hat{\Pi} \epsilon)^2 \right] \\ &= \mathbb{E}_{p_{e'}} \left[(\beta^{*T} \hat{\Pi} \Delta^T \epsilon)^2 \right] \\ &= \|\Delta \hat{\Pi} \beta^*\|^2. \end{aligned}$$

Next, the excess risk of the null vector $\hat{\beta} = \mathbf{0}$ in the same subspace is

$$\begin{aligned} \mathcal{R}_{p_{e'}}^{\hat{\Pi}}(\mathbf{0}) &= \mathbb{E}_{p_{e'}} [(\beta_{\hat{\Pi}}^{*T} \Sigma_{e'}^{-1/2} x)^2] \\ &= \mathbb{E}_{p_{e'}} [(\beta^{*T} \hat{\Pi} \epsilon)^2] \\ &= \|\hat{\Pi} \beta^*\|^2. \end{aligned} \quad \square$$

Lemma C.4. For a fixed $\bar{\Sigma}$, choosing an environmental covariance $\Sigma_{e'}$ is equivalent to directly choosing the error terms $\Delta_1, \Delta_2, \Delta_{12}, \Delta_{21}$.

Proof. For a fixed $\bar{\Sigma}$, due to the unique definition of square root as a result of Assumption 5.1, the map $\Sigma_{e'} \rightarrow \Sigma_{e'}^{1/2} \bar{\Sigma}^{-1/2} - I$ is one-to-one. Recall that we can write

$$U_{\hat{\Pi}}^T \Delta U_{\hat{\Pi}} = \begin{bmatrix} \Delta_1 & \Delta_{12} \\ \Delta_{21} & \Delta_2 \end{bmatrix}$$

which defines a one-to-one map from Δ to the error terms. Since the composition of bijective functions is bijective, the claim follows. \square

D. Implementation Details

All features were learned by finetuning a ResNet-50 using the default settings and hyperparameter sweeps of the DOMAINBED benchmark (Gulrajani & Lopez-Paz, 2021). We extracted features from 3 trials, with 5 random hyperparameter choices per trial, picking the one with the best training domain validation accuracy. We used the default random splits of 80% train / 20% test for each domain.

Using frozen features, the cheating linear classifier was trained by minimizing the multinomial logistic loss with full-batch SGD with momentum for 3000 steps. We did not use a validation set.

For the main experiments, all datasets except DomainNet could fit entirely in memory, so all algorithms were trained using full-batch L-BFGS (Liu & Nocedal, 1989). We used the exact same optimization hyperparameters for all methods; the default learning rate of 1 was unstable when optimizing IRM, frequently diverging, so we lowered the learning rate until IRM consistently converged (which occurred at a learning rate of 0.2). Since the IRM penalty only makes sense with both a feature embedder *and* a classification vector, we used an additional linear layer for IRM, making the objective non-convex. Presumably due to their convexity for linear classifiers, all other methods were unaffected by this change. For all methods, we halted optimization once 20 epochs occurred with no increase in training domain validation accuracy; the maximum validation accuracy typically occurred within the first 5 epochs.

For DomainNet, we used the Adam optimizer (Kingma & Ba, 2015) with batchsize 2^{13} and learning rate $1e-3$ for all methods. Again, the only method that required hyperparameter tuning for convergence was IRM. We halted optimization after 200 epochs with no increase in training domain validation accuracy.

For stability when whitening (and because the number of samples per domain was often less than the feature dimension), in estimating $\hat{\Sigma}_e$ for each environment we shrank the sample covariance towards the identity. Specifically, we define $\hat{\Sigma}_e = (1 - \rho) \frac{1}{n} \sum_{i=1}^n x_i x_i^T + \rho I$, with $\rho = 0.1$. We found that increasing λ beyond ~ 1 had little-to-no effect on the accuracy, loss, *or* penalty of the DARE solution (see Appendix E for ablations). However, we did observe that choosing a very large value for λ (e.g., 10^5 or higher) could result in poor conditioning of the objective, with the result being that the L-BFGS optimizer took several epochs for the loss to begin going down. When using Adam, the loss started going down immediately, but convergence was slower.

E. Additional Experiments

Here we present additional experimental results. All values represent the mean of three trials, and all error bars (where present) display 90% confidence intervals calculated as $\pm 1.645 \frac{\hat{\sigma}}{\sqrt{n}}$. Note though that the results are not independent across methods, so simply checking if the error bars overlap is overly conservative in identifying methods which perform better.

E.1. Cheating Accuracy with Pretrained Features

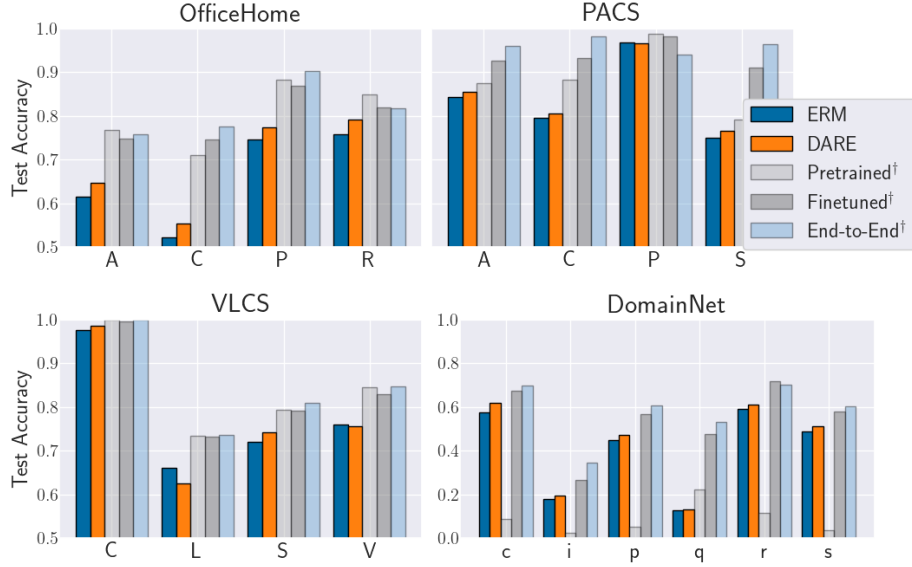


Figure 2. Recreation of Figure 1 cheating accuracy, but with the results of pretrained features included. We observe that the cheating linear classifier on top of pretrained features often still outperforms the ERM baseline by a large margin, though usually not by as much as the finetuned features. For DomainNet there is a clear need for finetuning, as the pretrained features are obviously insufficient for this task.

E.2. Ablations

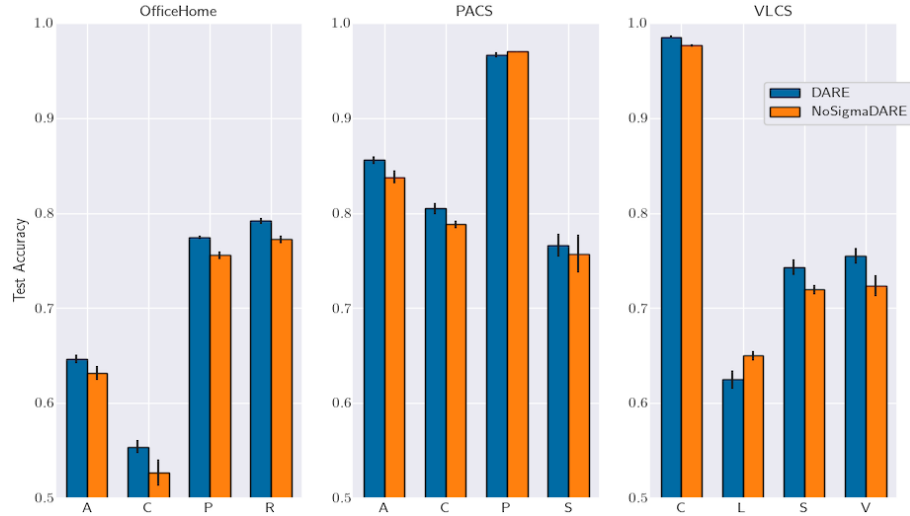


Figure 3. Demonstration of the effect of whitening. NoSigmaDARE is the exact same algorithm as DARE but with no covariance whitening. In almost all cases, covariance whitening + guessing at test-time results in better performance. We expect under much larger distribution shift that this pattern may reverse.

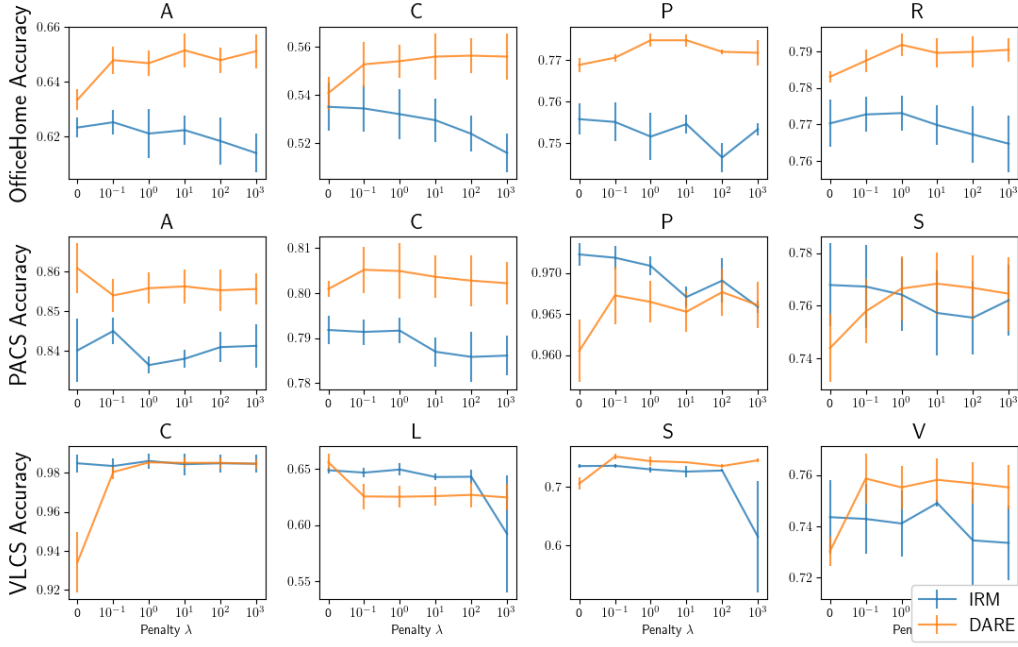


Figure 4. Effect of penalty term λ on the two algorithms which use it. DARE accuracy is extremely robust, effectively constant for all $\lambda \geq 1$; in practice we also found the penalty term itself to always be ~ 0 . In contrast, IRM accuracy appears to *decrease* with increasing λ , implying that the observed benefit of IRM primarily comes from the domain reweighting as in our GroupERM method.

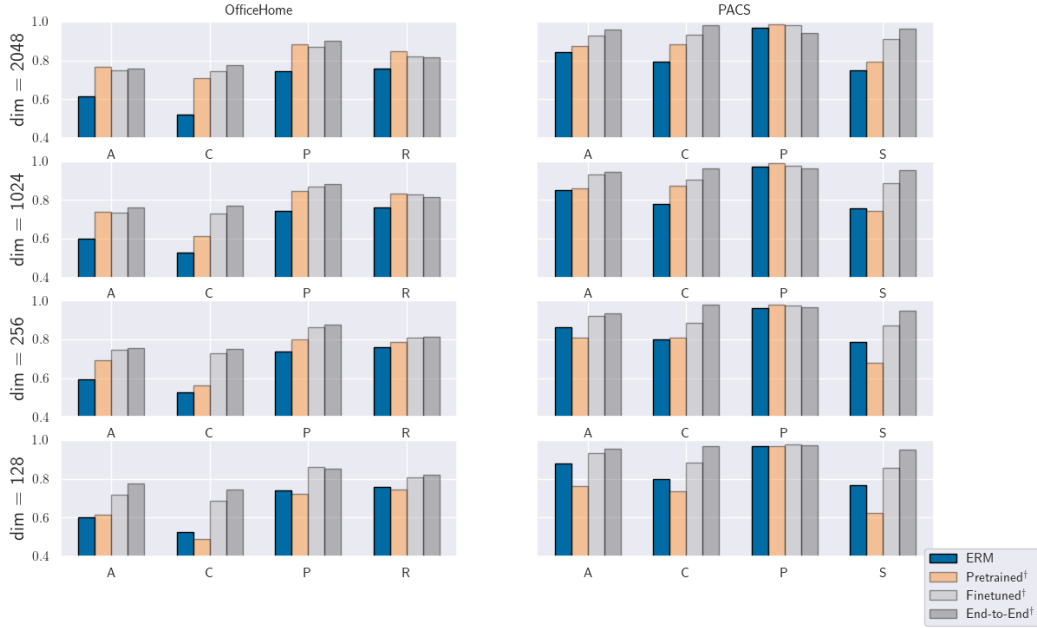


Figure 5. Effect of final feature bottleneck dimensionality on cheating accuracy. Reducing the dimensionality reduces accuracy of all methods to varying degrees, though in some cases it actually *increases* test accuracy. We observe that the main pattern persists, though the gap between cheating on finetuned features and traditional ERM shrinks as the dimensionality is reduced substantially. To reduce dimensionality of the pretrained features we use a random projection; unsurprisingly, the quality dramatically falls as the number of dimensions is reduced.